PHYSICAL REVIEW D VOLUME 44, NUMBER 4 15 AUGUST 1991

Billiard balls in wormhole spacetimes with closed timelike curves: Classical theory

Fernando Echeverria, Gunnar Klinkhammer, and Kip S. Thorne
Theoretical Astrophysics, California Institute of Technology, Pasadena, California 91125
(Received 27 February 1991)

The effects of self-interaction in classical physics, in the presence of closed timelike curves, are probed by means of a simple model problem: The motion and self-collisions of a nonrelativistic, classical billiard ball in a space endowed with a wormhole that takes the ball backward in time. The central question asked is whether the Cauchy problem is well posed for this model problem, in the following sense: We define the *multiplicity* of an initial trajectory for the ball to be the number of self-consistent solutions of the ball's equations of motion, which begin with that trajectory. For the Cauchy problem to be well posed, all initial trajectories must have multiplicity one. A simple analog of the science-fiction scenario of going back in time and killing oneself is an initial trajectory which is *dangerous* in this sense: When followed assuming no collisions, the trajectory takes the ball through the wormhole and thereby back in time, and then sends the ball into collision with itself. In contrast with one's naive expectation that dangerous trajectories might have multiplicity zero and thereby make the Cauchy problem ill posed ("no solutions"), it is shown that *all* dangerous initial trajectories in a wide class have *infinite* multiplicity and thereby make the Cauchy problem ill posed in an unexpected way: "far too many solutions." The wide class of infinite-multiplicity, dangerous trajectories includes all those that are nearly coplanar with the line of centers between the wormhole mouths, and a ball and wormhole restricted by (ball radius)$\ll$(wormhole radius)$\ll$(separation between wormhole mouths). Two of the infinity of solutions are slight perturbations of the self-inconsistent, collision-free motion, and all the others are strongly different from it. Not all initial trajectories have infinite multiplicity: trajectories where the ball is initially at rest far from the wormhole have multiplicity one, as also, probably, do those where it is almost at rest. A search is made for initial trajectories with zero multiplicity, and none are found. The search entails constructing a set of highly nonlinear, coupled, algebraic equations that embody all the ball's laws of motion, collision, and wormhole traversal, and then constructing perturbation theory and numerical solutions of the equations. A future paper (paper II) will show that, when one takes account of the effects of quantum mechanics, the classically ill-posed Cauchy problem ("too many classical solutions") becomes quantum-mechanically well posed in the sense of producing unique probability distributions for the outcomes of all measurements.

I. INTRODUCTION AND SUMMARY

A. Motivation

This is one of a series of papers that try to sharpen our understanding of causality by exploring whether the standard laws of physics can accommodate themselves, in a reasonable manner, to closed timelike curves (CTC's).

Previous papers have provided a natural spacetime arena for such an exploration: The arena of spacetimes that contain classical, traversible wormholes (i.e., multiply connected spatial slices). Morris, Thorne, and Yurtsever [1] showed that generic relative motions of the mouths of a traversible wormhole produce CTC's that loop through the wormhole's throat, and Frolov and Novikov [2] showed that generic gravitational redshifts at a wormhole's two mouths, due to generic external gravitational fields, also produce CTC's. (It is not clear whether the laws of physics permit the existence of such traversible wormholes; the attempt to find out is a separate line of research [1, 3–5], which we shall not discuss here.)

A consortium [6] of researchers from Moscow, Milwaukee, Chicago, and Pasadena (henceforth referred to as "the consortium") has raised the issue of whether the Cauchy problem is well posed in spacetimes with CTC's, and has explored many facets of the issue. This paper is one of several that elaborate on the ideas raised by the consortium [6].

Two examples of wormhole spacetimes with CTC's are depicted in Fig. 1. Both of these spacetimes are flat and Minkowski, except for the vicinity of the wormhole throat. The wormhole is arbitrarily short, and its two mouths move along two world tubes that are depicted as thick lines in the figure. The mouths are so small compared to their separation that one cannot see in the figure their finite size. Proper time τ at the wormhole throat is marked off along the mouths' world tubes; points with the same values of τ are the same event, on the throat, as seen through the two different mouths.

In Fig. 1(a) mouth 1 remains forever at rest, while mouth 2 accelerates away from 1 at high speed, then returns and decelerates to rest. Because the motions of the two mouths are like those of the twins in the standard special-relativistic twin paradox, we shall refer to this as the "twin-paradox spacetime." The same relative aging as occurs in the twin paradox produces, here, closed timelike curves that loop through the wormhole [1]. The

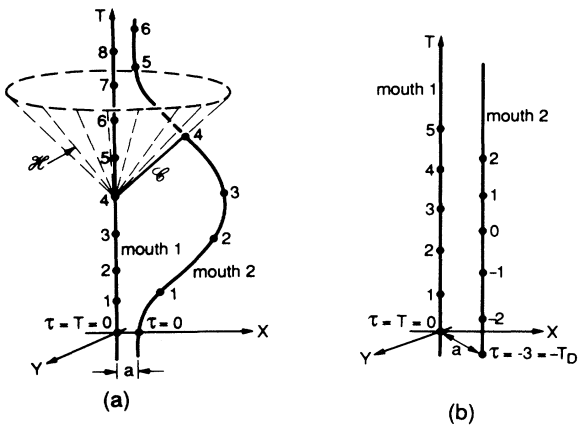

FIG. 1. Two examples of wormhole spacetimes with closed timelike curves. (a) The "twin-paradox spacetime," (b) the "eternal-time-machine spacetime."

light-cone-like hypersurface $\mathcal{H}$ shown in the figure is a Cauchy horizon. Through every event to the future of this Cauchy horizon $\mathcal{H}$ there are CTC's; nowhere in the past of $\mathcal{H}$ are there any CTC's.

In Fig. 1(b) the two mouths are both forever at rest, but with a time delay T_d between them that is greater than the distance a separating them. Because there are CTC's looping through the wormhole throughout this spacetime, the wormhole can be used in principle as a "time machine" for traveling arbitrarily far into the past or the future. For this reason, it has become conventional to call this the "eternal-time-machine spacetime."

Many aspects of the twin-paradox spacetime and the eternal-time-machine spacetime have been studied elsewhere in the literature [1, 6, 3, 7]. Most importantly for us, the consortium [6], and Friedman and Morris [7] have used these spacetimes as "testbed arenas" for studying whether the Cauchy problem is well posed in the presence of CTC's.

As the consortium has shown [6], it is an exceedingly delicate enterprise to pose initial data in a region of spacetime that is threaded by CTC's (the region to the future of the Cauchy horizon in the twin-paradox spacetime; anywhere, except past null infinity, in the eternal-time-machine spacetime). The delicacy is caused by the absence of well-behaved spacelike or null hypersurfaces in such a region, on which to pose the data. Various aspects of this delicacy are discussed by the consortium [6] and by Yurtsever [8], and we shall not in this paper attempt to elucidate them further. Rather, we shall confine attention to the more straightforward situation of initial data that are posed in regions to the past of all CTC's; i.e., data posed on a spacelike or null Cauchy surface to the past of the Cauchy horizon $\mathcal{H}$ in the twin-paradox spacetime, and data posed on past null infinity in the eternal-time-machine spacetime. We shall ask (as did the consortium [6]) whether the Cauchy problem is well posed for such initial data, in the following sense: If one gives the same standard initial data as one would do in a spacetime without CTC's, then for each choice of those data does there exist a self-consistent, global solution of the standard, local evolution equations, and if so is the self-consistent solution unique? (The demand for self-consistency has been discussed in depth by the consortium [6].)

One can ask about the well posedness of the Cauchy problem for a variety of types of evolving systems in spacetimes with CTC's. The first step, carried out by Friedman and Morris [7], was to study the evolution of a classical, massless scalar field ϕ. Friedman and Morris showed rigorously that the Cauchy problem is well posed for such a field in the eternal-time-machine spacetime: Every arbitrary initial value of the field $r\phi$ (where r is radial distance), posed at past null infinity (limit as $T-r \to -\infty$), gives rise, via the standard local evolution equation $\Box\phi = 0$, to a unique, globally self-consistent field ϕ throughout the eternal-time-machine spacetime. It seems highly likely that this behavior is prototypical in the sense that, for any zero-rest-mass, noninteracting, classical field (e.g., the vacuum electromagnetic field) in any stable wormhole spacetime with CTC's, the Cauchy problem will be well posed [1, 6, 7].

It seems probable that the well posedness of the Cauchy problem for the field ϕ results from the fact that ϕ has no self-interactions. More likely to produce peculiar results is a system that, after traveling around a nearly closed timelike world line, can interact with its younger self (e.g., a person who tries to kill his younger self). The simplest such classical system is a single, classical particle that carries a hard-sphere, repulsive potential and has no internal degrees of freedom (a "billiard ball"), and that travels with a speed small compared to light so special-relativistic effects can be ignored. The purpose of this paper is to study the Cauchy problem for such a billiard ball in the twin-paradox and the eternal-time-machine spacetimes.

Other papers in this series study the well posedness of the Cauchy problem for systems that embody other pieces of physics: A companion paper to this one (paper II [9]) studies the effects of nonrelativistic quantum mechanics on the Cauchy problem for this paper's billiard ball; Novikov and Petrova [10] are currently studying a classical billiard ball that has huge numbers of internal degrees of freedom and thus can behave inelastically when it collides with itself; and Novikov [11] has examined, semiquantitatively, a number of complicated classical systems (e.g., a bomb that explodes in response to a trigger signal, sending explosive debris through a wormhole and backward in time where it tries to trigger the explosion before the explosion actually occurs). For his complicated classical systems, Novikov shows that it is *plausible* that there always exists at least one self-consistent solution, no matter how paradoxical the initial data may appear. Unfortunately, for such complicated systems it seems hopeless to obtain firm results. Accordingly, in this paper, in a quest for firmness, we examine the simplest system we can think of that has self-interactions: the perfectly elastic, nonrelativistic billiard ball.

B. The Cauchy problem for classical billiard balls

In this paper we pose our initial data (initial billiard ball *trajectory*, by which we mean *initial path and speed*), in the region of spacetime that is devoid of CTC's: before the Cauchy horizon for the twin-paradox spacetime [Fig. 1(a)], or at past null infinity for the eternal-time-machine spacetime [Fig. 1(b)]. For the twin-paradox spacetime, we confine attention for simplicity to initial trajectories that take the ball into the vicinity of the wormhole long after mouth 2 has returned to rest. This permits us, throughout the calculation, to ignore the early-time, relative motion of the wormhole mouths and to treat the twin-paradox spacetime as though it were the same as the eternal-time-machine spacetime, i.e., the same as Fig. 1(b).

The structure of this (common) spacetime can be understood easily as follows [6]: Take ordinary, flat, Minkowski spacetime, cut out of it the world tubes of two balls that are at rest in a chosen Lorentz coordinate system (T, X, Y, Z), and identify the surfaces of the balls, with a time delay T_d between them. The surfaces of the two balls are the mouths of the wormhole, and because they have been identified with each other, the wormhole is vanishingly short.

We shall denote by D the separation between the centers of the two mouths as measured in the Lorentz frame where they are at rest, by b the radii of the two mouths (radius of curvature of their surfaces), by T_d the time delay between the two mouths, and by r the radius of the billiard ball. Throughout this paper we shall measure spatial distances in units of D (so the wormhole mouth separation is unity) and times in units of T_d (so the time delay between the two mouths is unity); and we shall denote by $B \equiv b/D$ and $R \equiv r/D$ the wormhole radius and the billiard ball radius, measured in these units, and by v the billiard ball speed, measured in these units (units of D/T_d).

The identification we shall use for the two wormhole mouths is one in which diametrically opposed points (points obtained by reflection in the plane half way between the two mouths) are identical. Stated more pedestrianly (see Fig. 2): Adjust the Lorentz frame's spatial, Cartesian coordinates so the line of centers between the two mouths lies on the X axis. Then set up a right-handed spherical polar coordinate system (Θ, Φ) on the right mouth with the polar axis pointed in the $-X$ direction (along the line of centers, toward the left mouth) and with $\Phi = 0$ along the $-Y$ direction; and set up a left-handed spherical polar coordinate system (Θ, Φ) on the left mouth with polar axis pointed in the $+X$ direction (along the line of centers, toward the right mouth) and with $\Phi = 0$ along the $-Y$ direction. Then points on the two mouths with the same values of Θ and Φ are identified.

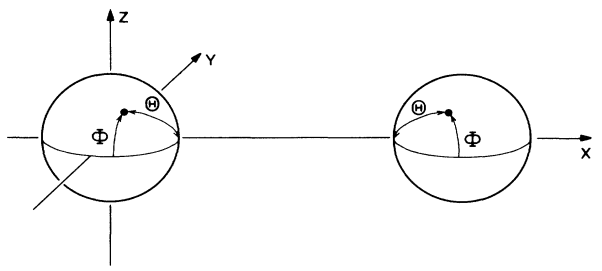

FIG. 2. The identification of points on the two mouths of the wormhole.

In our study of the Cauchy problem for a billiard ball in the above spacetime, we shall focus on the issue of the *multiplicity* of solutions to the ball's equations of motion. For each initial trajectory (initial path and speed) we define the multiplicity to be the number of self-consistent solutions of the equations of motion that begin with that trajectory. Not surprisingly, it will turn out that each initial trajectory has a discrete set of solutions, and thus has multiplicity zero or one or two or .... In the absence of CTC's, all trajectories have multiplicity one, which is just a fancy way of saying that the Cauchy problem is well posed. From exposure to science-fiction scenarios (e.g., those in which one goes back in time and kills oneself), one might expect CTC's to give rise to initial trajectories with zero multiplicity—a severe form of ill posedness for the Cauchy problem. However, we have searched hard for initial trajectories with zero multiplicity and have found none. On the other hand, our search has not covered all initial trajectories (see especially Sec. V), so we cannot guarantee the nonexistence of zero-multiplicity trajectories.

The only trajectories that have any possibility for zero multiplicity are those which, when followed assuming no collision, produce a collision. We call such trajectories *dangerous*. A trajectory can be dangerous only if it leads the ball into the wormhole, and this can happen only if the trajectory is nearly coplanar with the line that connects the centers of the wormhole mouths—more specifically, only if it is within a distance $B =$ (mouth radius) of being coplanar with the line of centers. For this reason, in this paper we restrict attention to nearly coplanar trajectories. The analysis of the billiard ball motion is fairly manageable when the initial trajectory is precisely coplanar (Secs. II, III, and IV); and the *slightly* noncoplanar case (within a distance $\ll B$ of coplanar) can be treated using perturbation theory (Sec. V). However, we have not found a manageable way to analyze the case of coplanarity to within a distance $\sim B$.

For the slightly noncoplanar case, and for $R \ll B \ll D \equiv 1$ (ball small compared to mouths and mouths small compared to separation of mouths), we shall derive a rather remarkable result (Sec. IV A): *All dangerous initial trajectories have infinite multiplicity.* What a contrast with one's naive, science-fiction-based expectation of zero multiplicity.

Figure 3 gives insight into two of the infinite set of solutions in the precisely coplanar case. Figure 3(a) is the self-inconsistent solution which tells us that the initial trajectory, labeled α, is dangerous. When, as in Fig. 3(a), we assume that the ball travels freely along α without suffering a collision, it passes through the wormhole, emerges along β before it went in, and hits itself so hard that it knocks itself along α', preventing itself from go-

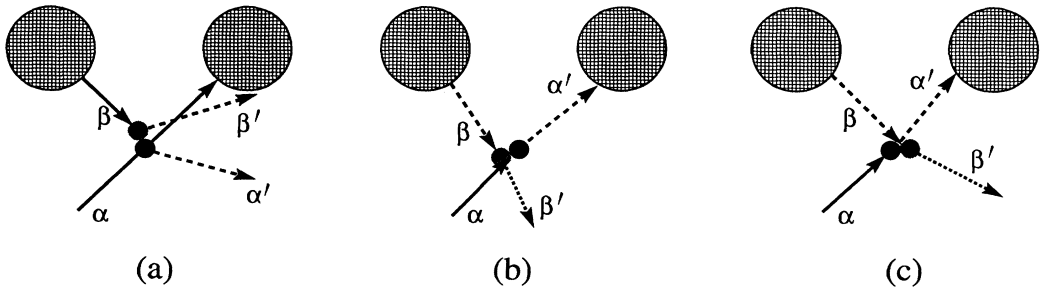

FIG. 3. Spatial diagrams showing a prototypical example of initial data that produce two self-consistent solutions to the billiard-ball equations of motion. Each diagram shows the ball's spatial trajectory, and also shows the ball itself (young version in black and old version in grey) at the moment of self-collision. (a) The self-inconsistent solution which arises if one assumes the ball does not get hit before traversing the wormhole. (b) A "class-I" self-consistent solution in which the ball is speeded up and deflected rightward slightly by a collision before entering the wormhole. (c) A "class-II" self-consistent solution in which the ball is slowed and deflected leftward slightly by a collision before entering the wormhole.

ing through the wormhole. Figure 3(b) is what we call a "self-consistent solution of *class I*" for this same initial trajectory α. The ball, while traveling toward the wormhole on α, gets hit gently on its left rear side and is speeded up a bit and deflected rightward a bit (along trajectory α'); it then enters the wormhole and reemerges before it went down (trajectory β), it tries to pass behind its younger self, but gets hit a gentle, glancing blow by its younger self and deflected slightly (along trajectory β'). Figure 3(c) is what we call a "self-consistent solution of *class II*." While traveling toward the wormhole, the ball (trajectory α) gets hit gently on its front right side and is slowed a bit and deflected leftward a bit (along trajectory α'), it enters the wormhole and reemerges before it went down (trajectory β), it passes in front of its younger self and, just before getting all the way past, it gets hit a gentle, glancing blow by its younger self and deflected slightly (along trajectory β'). We shall study the details of such coplanar class-I and class-II solutions in Sec. IV and in Appendixes A and B—and shall do so not only for $R \ll B \ll D \equiv 1$, but also for wormholes with large mouths and balls with large radii.

The class-I and class-II solutions are small perturbations of the self-inconsistent solution, in the sense that the ball's path is displaced by only enough (typically of order the ball's radius R) to permit the ball to undergo a glancing collision rather than a head-on collision. By contrast, the other self-consistent solutions are quite different from the self-inconsistent one. They (or at least the ones studied in this paper) involve a collision that occurs somewhat farther from the wormhole than for class I and class II, and correspondingly the distance the ball travels, from its first encounter with the collision to its second, is rather larger than in the class-I and class-II solutions. This means the ball must travel farther back in time to achieve such a solution. It does so by undergoing several wormhole traversals. In Sec. III we shall exhibit a self-consistent solution corresponding to each value of the integer $n \equiv$ (number of wormhole traversals); and we shall do so not only when the initial trajectory is dangerous, but in fact for almost all coplanar initial trajectories with speeds $v_1 > D/T_d \equiv 1$. Figure 9 (in Sec. III) is an example with eight traversals.

Our analysis of these multiple-traversal solutions, by contrast with our analysis of the class-I and class-II solutions, is restricted to $R \ll B \ll D \equiv 1$. This restriction permits us to ignore the details of the balls' relative geometry during the collision event (aside from proving, in Sec. II, that the necessary geometry exists). By decoupling the details of the collision geometry from the rest of the solution, we bring the multiple-traversal analysis into an elegant geometric form that contrasts with the complicated algebraic calculations used to analyze the class-I and class-II solutions. This difference motivates our presenting the multiple-traversal analysis (Sec. III) before the class-I–class-II analysis (Sec. IV).

This paper restricts attention, for simplicity, to solutions that entail a single self-collision. There presumably are also multiple-collision solutions, and we speculate about some possible, rather strange ones in the paragraph containing Eq. (3.11). Such solutions can only increase the tendency of initial trajectories to have high, even infinite, multiplicity.

Having identified this tendency toward high multiplicity, we ask ourselves in Sec. III C whether there exist any solutions with multiplicity 1; and in Secs. IV and V, whether there exist any with multiplicity zero. Our search for multiplicity zero comes up empty handed; all initial trajectories that we have examined have self-consistent solutions. By contrast, there is *at least* a small (measure-zero) class of initial trajectories with unit multiplicity: those in which the ball is initially at rest far from the wormhole. We suspect, but have not proved, that the (finite-measure) initial trajectories with speeds $v_1 \ll D/T_d \equiv 1$ and with impact parameters $h \gg D \equiv 1$ also have unit multiplicity; see Sec. III.

The above conclusions are derived for the precisely coplanar case in Secs. II, III, and IV; and they then are all extended to the slightly noncoplanar case in Sec. V. This extension is accomplished by demonstrating (via perturbation theory) that for each slightly noncoplanar initial trajectory there is a one-to-one correspondence between its self-consistent solutions and those of a nearby, precisely coplanar initial trajectory.

This paper's principal conclusion, that the Cauchy problem is ill posed for classical billiard balls in the

eternal-time-machine spacetime, suggests at first sight that the laws of physics might not be able to accommodate themselves in any reasonable way to CTC's. However, the laws of classical mechanics are only an approximation to the more fundamental laws of quantum mechanics, and in paper II [9] it will be shown that quantum mechanics can cure the multiple-solution ill posedness (and can also cure a zero-multiplicity ill posedness, if it occurs): For each initial quantum state of a nonrelativistic billiard ball, posed before the region of CTC's, the sum-over-histories formulation of quantum mechanics predicts unique probabilities for the outcomes of all sets of measurements that one might make in the region of CTC's.

C. Outline of this paper

We begin our quantitative analysis of coplanar solutions in Sec. II, by laying some foundations. In Sec. II A we derive simple "wormhole traversal" rules for the change of a billiard ball's velocity when it goes through the wormhole. Then in Sec. II B we analyze the kinematics of a billiard ball's self-collision when there is only one collision event along the ball's world line. Our analysis simplifies subsequent calculations by embodying all the kinematics (energy conservation, momentum conservation, and friction-free billiard-ball contact at the collision event) in one simple rule: the collision must produce either a direct "velocity exchange," or a "mirror exchange" of velocities.

In Sec. III, by combining the wormhole traversal rules with velocity-exchange and mirror-exchange collisions, and restricting attention to $R \ll B \ll D \equiv 1$, we show that multiple solutions to the billiard ball's equations of motion are ubiquitous. More specifically, we show that a finite measure of such (coplanar) initial trajectories produce not only multiple solutions (Sec. III A), but in fact an infinity of solutions (infinite multiplicity; Sec. III B). We then show that *not all* initial trajectories have infinite multiplicity; there do exist some with only one solution (unit multiplicity; Sec. III C).

In Sec. IV we turn our attention to *dangerous*, coplanar initial trajectories. We begin in Sec. IV A by proving, as a corollary of the Sec. III B analysis, that for $R \ll B \ll D \equiv 1$ almost all such trajectories have infinite multiplicity. Then we extend our search for multiplicity zero to balls that are large enough for the geometry of the collision to couple significantly into the rest of the solution, $R \not\ll B$. In Appendix A and Sec. IV B we derive a set of highly nonlinear, coupled equations governing self-consistent solutions with such collisions. Those equations are valid not only for $R \not\ll B$, but also for $B \not\ll D \equiv 1$. However, in Appendix B and Sec. IV C we return to the restriction $B \ll D$ and there search for solutions of the equations. We find analytic, perturbation-theory solutions of classes I and II for almost all initial trajectories; and we construct numerical solutions for some typical initial trajectories in the extreme regions where the perturbation-theory solutions fail. Our spot checks in these extreme regions have not turned up any initial trajectories for which numerical solutions do not exist.

In Sec. V, using perturbation theory, we extend to slightly noncoplanar initial trajectories all the coplanar results of the previous sections.

II. FOUNDATIONS: WORMHOLE TRAVERSALS AND SELF-COLLISIONS

In this section we give brief analyses of coplanar wormhole traversals and billiard-ball self-collisions—analyses that produce simple rules for use in subsequent sections.

A. Coplanar wormhole traversals

For nearly all the wormhole traversals encountered in this paper, the ball's trajectory is coplanar with the line of centers of the wormhole mouths, and the ball enters mouth 2 and exits from mouth 1, thereby traveling backward in time. In this section we shall confine attention to such traversals.

For all traversals, we shall presume that the ball is small enough (ball radius R sufficiently small compared to mouth radius B) that we can ignore the impulsive tidal force exerted on the ball's hard-sphere potential by the concentrated spacetime curvature at the wormhole throat. Just how small R must be for this depends on one's model for the internal structure of the ball.

In this paper our model for the ball will have the following features. (i) We shall refuse to consider collisions that occur while the center of the ball is on one side of the wormhole throat and its colliding surface is on the other; thereby we shall avoid worrying about instantaneous tidal deformations of the ball's hard-sphere potential during the traversal. (ii) We shall assume (for simplicity and definiteness) that, even if R is as large as, say, $B/2$, the ball's center moves through the wormhole in the same manner as would an arbitrarily small ball. (iii) We shall assume that, even for R as large as $B/2$, the ball recovers from its tidal distortions and resumes its radius-R, spherical shape arbitrarily quickly after a traversal. These features of our model are sufficient to permit R to be as large as $B/2$. (Our choice of $B/2$ rather than $B/4$ or $9B/10$ is quite arbitrary.)

Since the ball's center moves through the wormhole in the same manner as would an arbitrarily small ball, its motion must be on a straight line and with constant speed, as seen by an observer at rest on the throat. Such motion guarantees energy and momentum conservation during the traversal, as seen by the observer. (We presume that the wormhole recoils negligibly; i.e., we treat the ball as a "test object" that moves through the fixed wormhole geometry.)

Since the wormhole mouths are both at rest in the external space, constant speed as seen on the throat implies that the speed of the ball, as measured in the exterior, is unchanged by the traversal: $v_{\rm out} = v_{\rm in}$.

Straight-line motion, as measured on the throat, implies that the ball's outgoing velocity $\mathbf{v}_{\rm out}$ makes the same angle θ, with the outgoing mouth's outward normal, as the ball's ingoing velocity $\mathbf{v}_{\rm in}$ makes with the ingoing mouth's inward normal. This in turn implies (cf. Fig. 4) that the angle ψ from the mouths' line of centers

(the X axis) to the ball's velocity vector changes during the wormhole traversal from $\psi = \theta + \phi$ to $\psi = \theta - \phi$. Here ϕ is the angular location of the traversal on the wormhole throat as depicted in Fig. 4 (not to be confused with the Φ of Fig. 2).

These conclusions are summarized by the following "wormhole traversal rules":

$$v_{\rm out} = v_{\rm in} \ , \tag{2.1a}$$

$$\psi_{\rm out} = \psi_{\rm in} - 2\phi \ . \tag{2.1b}$$

Here and throughout, an italic v denotes the magnitude (speed) of the velocity $\mathbf{v}$.

B. Coplanar self-collisions

In this section and throughout this paper we restrict attention to self-consistent solutions that involve a single self-collision. We shall denote by $\mathbf{v}_1$ the ball's velocity as it enters the collision the first time, by $\mathbf{v}_1'$ its velocity as it leaves the collision the first time, by $\mathbf{v}_2$ its velocity as it enters the second time, and by $\mathbf{v}_2'$ its velocity as it leaves the second time. In other words, the sequence of velocities as measured by the ball itself is $\mathbf{v}_1$, $\mathbf{v}_1'$, $\mathbf{v}_2$, $\mathbf{v}_2'$.

No matter how many wormhole traversals the ball may make between its two visits to the collision event, the "speed in equals speed out" wormhole traversal rule implies that

$$v_1' = v_2 \ ; \tag{2.2a}$$

and this, combined with energy conservation, implies that

$$v_2' = v_1 \ . \tag{2.2b}$$

These two speed relations, together with the collision's law of momentum conservation,

$$\mathbf{v}_1' + \mathbf{v}_2' = \mathbf{v}_1 + \mathbf{v}_2 \ , \tag{2.2c}$$

are a complete set of conservation laws for the ball's velocity.

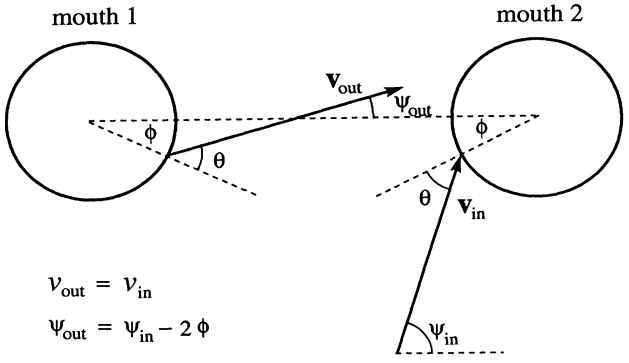

FIG. 4. The "wormhole traversal rules" [Eqs. (2.1)], which govern coplanar wormhole traversals from mouth 2 to mouth 1.

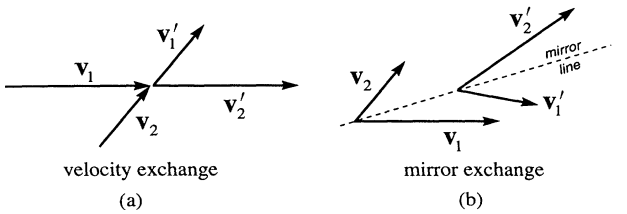

FIG. 5. The two solutions to the self-collision equations: "velocity exchange" [Eq. (2.3a)], and "mirror exchange" [Eq. (2.4a)].

These conservation laws can be satisfied in precisely two ways (Fig. 5): (i) *velocity exchange*,

$$\mathbf{v}_1' = \mathbf{v}_2, \quad \mathbf{v}_2' = \mathbf{v}_1 \ , \tag{2.3a}$$

for which the relative position of the balls at the moment of collision (the vector separation of their centers) is

$$\mathbf{r}_1 - \mathbf{r}_2 = 2R\frac{\mathbf{v}_2 - \mathbf{v}_1}{|\mathbf{v}_2 - \mathbf{v}_1|} \ ; \tag{2.3b}$$

and (ii) *mirror exchange*,

$$\begin{aligned} \mathbf{v}_1' &= (\mathbf{v}_2)_{\text{reflected in line parallel to } \mathbf{v}_1+\mathbf{v}_2} \ , \\ \mathbf{v}_2' &= (\mathbf{v}_1)_{\text{reflected in line parallel to } \mathbf{v}_1+\mathbf{v}_2} \ , \end{aligned} \tag{2.4a}$$

for which the relative position of the balls at the moment of collision is

$$\mathbf{r}_1 - \mathbf{r}_2 = 2Rs\frac{\mathbf{v}_2 + \mathbf{v}_1}{|\mathbf{v}_2 + \mathbf{v}_1|}, \tag{2.4b}$$

where $s = \text{sign}(v_2 - v_1)$. [The relative position of the balls when they collide, Eq. (2.3b) or (2.4b), is determined by the fact that the momentum transfer $\mathbf{v}_1' - \mathbf{v}_1$ must be along the balls' line-of-centers direction $\mathbf{r}_1 - \mathbf{r}_2$, and the centers must be separated by a distance $2R$.]

In summary, all the constraints on velocity that a self-collision must satisfy are embodied in the simple statement that *either the balls undergo velocity exchange* (2.3a), *or they undergo mirror exchange* (2.4a).

III. UBIQUITY OF MULTIPLE SOLUTIONS FOR COPLANAR INITIAL TRAJECTORIES

In this section we shall use the geometry of the velocity exchange, mirror exchange, and wormhole traversal rules to show that multiple solutions to the billiard ball's equations of motion are ubiquitous. Our discussion will be confined to coplanar initial data. However later, in Sec. V, we shall see that all coplanar solutions are stable (continue to exist) when one perturbs the initial data in an arbitrary but infinitesimal, noncoplanar way. In our discussion, as in Sec. I, we shall refer to the number of solutions that an initial trajectory produces as its "multiplicity."

We begin in Sec. III A by showing that all coplanar initial trajectories that are aimed between the wormhole mouths have multiplicity at least two. One solution is unperturbed straight-line motion, and a second is com-

posed of a wormhole traversal and a velocity-exchange collision. Then in Sec. III B we show that there is a wide variety of coplanar initial trajectories (a set of finite measure) with infinite multiplicities. Each of the solutions we exhibit, for these initial trajectories, has a single mirror-exchange collision, together with some number n of wormhole traversals; n ranges over positive integers up to infinity. Finally, in Sec. III C, we show that a ball initially at rest far from the wormhole has only one solution to its equations of motion: the trivial solution where it remains forever at rest. We also argue, but do not prove firmly, that there is only a single solution for any ball with (i) an initial speed that is sufficiently slow but not zero, and (ii) an initial path of motion that, if extended forever, remains far from the wormhole.

A. Multiplicity larger than 1 is generic

Consider a ball whose initial path is coplanar with the mouths' line of centers and is directed between the mouths, and whose initial speed is arbitrary but nonzero. An obvious solution to the ball's equation of motion is collision-free, wormhole-traversal-free, straight-line motion [Fig. 6(a)]. A second solution is shown, for the case of an arbitrarily small ball, in Fig. 6(b). The ball is hit as it crosses the mouths' line of centers and gets knocked radially into mouth 2. Regardless of the ball's initial speed v_1, it is hit with just the right impulse to give it a speed $v_1' = (D - 2B)/T_d \equiv 1 - 2B$. It travels through the wormhole and returns to its impact point at just the right moment to hit itself and be deflected back onto its

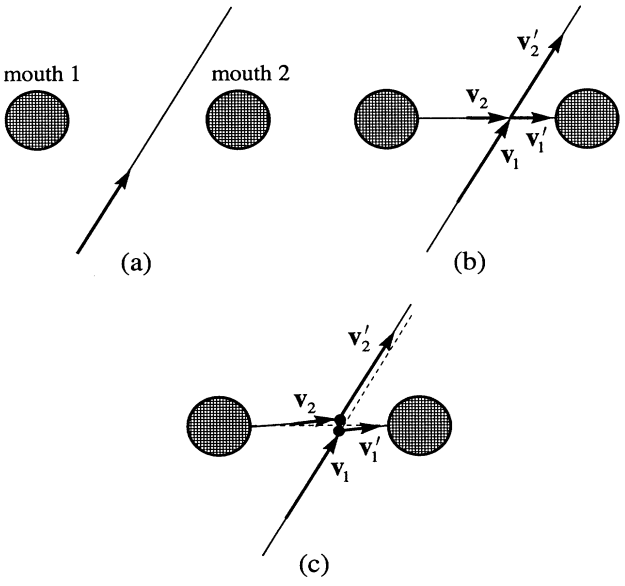

FIG. 6. Solutions to the equations of motion for a coplanar initial trajectory that is directed between the wormhole mouths. The ball's speed is arbitrary. (a) The trivial solution. (b) A solution with one wormhole traversal and a velocity-exchange collision. (c) Modification of solution (b) when the radius of the ball is not negligible.

original trajectory. Since the wormhole traversal rules (2.1) are trivially obeyed, and the ball has obviously undergone a velocity-exchange collision, all the equations of motion are satisfied.

If the ball's radius is not arbitrarily small, both solutions, (a) and (b), still exist. However, the details of solution (b) are modified slightly, as shown in (c). The collision still entails a precise velocity exchange, and the wormhole traversal rule is still satisfied (but not quite so trivially as before). However, there is now an offset of the various pieces of the ball's path (solid lines) relative to the previous path (dotted lines).

It is not hard to convince oneself that, when the ball is given a finite but small size $R \ll B$, all the solutions described in the remainder of Sec. III remain valid with tiny modifications similar to those in Fig. 6(c). However, for ease of presentation we henceforth in Sec. III shall keep the ball's size infinitesimal.

B. Infinite multiplicity is generic

As a first step in demonstrating that infinite multiplicity is generic (i.e., that all the initial trajectories in a set of finite measure have infinite multiplicity), consider the highly symmetric initial trajectory shown in Fig. 7. The ball's initial speed is arbitrary, and its initial path is coplanar with and perpendicular to the line of centers and is directed half way between the two mouths. Figures 7(a)–7(d) are four self-consistent solutions for this initial trajectory, and they obviously are generalizable to produce an infinite set of solutions. Yet another solution is that of Fig. 6(b), which involves velocity exchange by contrast with the mirror exchange of Fig. 7.

The solution shown in Fig. 7(b) was pointed out to us by Forward [12] (and it motivated our discovery of the infinite multiplicity of solutions). In this solution the ball experiences a mirror-exchange collision, which knocks it radially into mouth 2. It then emerges radially from mouth 1, earlier in external time by precisely the right amount $T_d = 1$ to enable it to return to the collision event. The wormhole-traversal rules (2.1) are trivially satisfied ($\psi_{\rm in} = \phi$, $\psi_{\rm out} = -\phi$; $v_1' = v_2$), and the mirror-exchange rule is satisfied with the mirror line parallel to the line of centers (horizontal dashed line). Since the mirror line must be along $\mathbf{v}_1 + \mathbf{v}_2$, the speed v_2 must be $v_2 = v_1/\sin\psi$ (where ψ, as shown in the figure, is the $\psi_{\rm in}$ of the wormhole-traversal rule). The total distance traveled by the ball between collisions (in the limit, for simplicity, that $B \ll 1$) is $1/\cos\psi$, so the total time lapse as measured by the ball between collisions is $(1/\cos\psi)(1/v_2) = \tan\psi/v_1$. This ball-measured time lapse must be equal to the amount of backward time travel, $T_d = 1$, during the ball's wormhole traversal, in order that the ball return to the collision event. Correspondingly, the value of ψ must be given by

$$\tan\psi = v_1 \ . \tag{3.1}$$

Notice that there is no constraint whatsoever on the initial speed v_1. All the equations of motion are satisfied in Fig. 7(b), when ψ has the value (3.1), regardless of

how large or how small v_1 might be.

In the limit as v_1 goes to zero, the ball is initially at rest on the mouths' line of centers; it gets hit and knocked radially into mouth 2 at speed $v_2 = 1$; it travels backward in external time by $T_d = 1$ while traversing the wormhole; and it then emerges radially from mouth 1, travels to the collision event, hits itself, and comes to rest. Note that this solution is really a continuous infinity of solutions: the time T of the collision is completely arbitrary.

The solution in Fig. 7(c) involves two wormhole traversals. As measured by the ball, using its own local time, the sequence of events is the following: (i) initial path α, (ii) mirror-exchange collision, (iii) path β from collision to mouth 2, (iv) first wormhole traversal, (v) path γ from mouth 1 to mouth 2, (vi) second wormhole traversal, (vii) path δ from mouth 1 to collision event, (viii) path ε (opposite to initial path).

As seen by external observers, the sequence is quite different. It is straightfoward to verify, by the same method as was used in solution (b), that in the limit $B \ll 1$ the angle ψ is given by

$$\sin\psi + \tan\psi = 2v_1 \ , \tag{3.2}$$

and that the sequence of events is as follows. (i) At time $T = -1/(1+\cos\psi)$ before the collision, the ball emerges from mouth 1 and starts traveling along δ toward the collision event, while (in its younger incarnation) it is also traveling up α. (ii) At time $T = -\cos\psi/(1+\cos\psi)$, the ball emerges from mouth 1 and starts traveling along γ toward mouth 2; there are now three incarnations of the ball present. (iii) At time $T = 0$, the collision between incarnations α and δ occurs, knocking incarnation α along β and incarnation δ along ε; the third incarnation is still traveling along γ. (iv) At $T = \cos\psi/(1+\cos\psi)$, the ball on γ enters mouth 2 and disappears, leaving just two balls: one on ε, the other on β. At $T = 1/(1+\cos\psi)$, the ball on β enters mouth 2 and disappears, leaving just one ball, traveling along the final trajectory ε.

Figure 7(d) involves three wormhole traversals. The sequence of paths as measured by the ball is in Greek alphabetical order. It is left as an exercise for the reader to compute the angle ψ in the limit $B \ll 1$ and compute the detailed timings of events as seen by external observers. The reader should also be able to verify (perhaps with the aid of Fig. 9 below and the associated discussion) that the wormhole-traversal rules and mirror-exchange rules are satisfied.

The generalization of the solutions of Fig. 7 to an arbitrarily high number of wormhole traversals should be obvious. We shall examine, in Fig. 9 below, the details of the sequence of wormhole traversals involved in that generalization.

The generalization of these mirror-exchange solutions to arbitrary coplanar initial trajectories is not quite so easy as in the velocity-exchange case of Fig. 6. The method of generalization, for a one-traversal solution, is shown in Fig. 8. The steps in the method are as follows: (i) Specify the initial path α, but not the initial speed v_1; the initial speed will be calculated as the last step in the method. Specify, instead of the initial speed, the location P along the initial trajectory α at which the collision occurs. (ii) By trial and error find a path that takes the

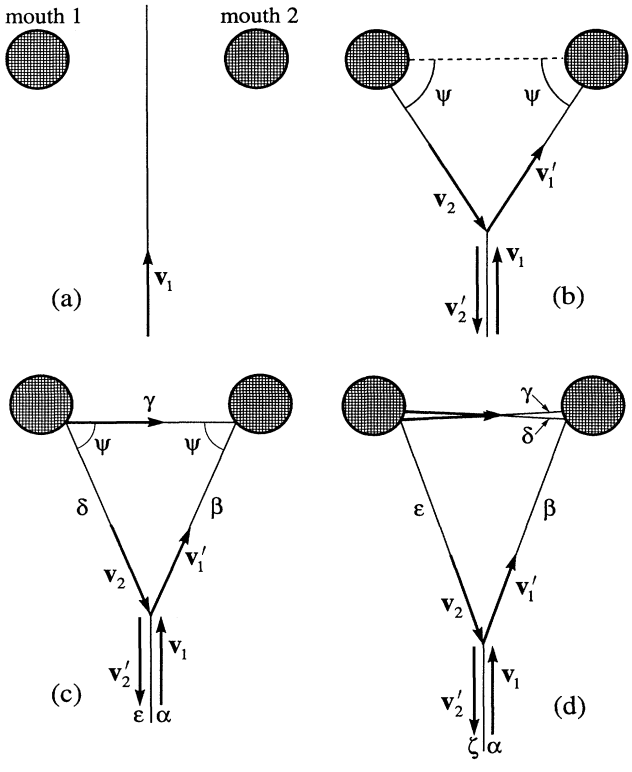

FIG. 7. A specific example of an initial trajectory with an infinite number of solutions (infinite multiplicity). (a) The trivial solution. (b) Solution with one mirror-exchange collision and one wormhole traversal. (c) Solution with one mirror-exchange collision and two wormhole traversals. (d) Solution with one mirror-exchange collision and three wormhole traversals. Solution (b) was pointed out to us by Forward [12] and motivated our discovery of solutions (c) and (d) and their generalizations.

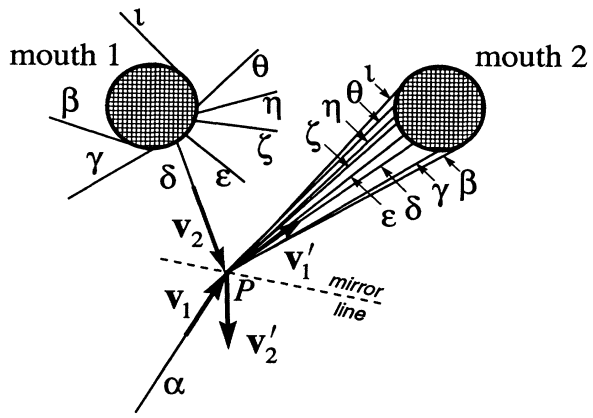

FIG. 8. Trial-and-error method of generating a one-traversal, mirror-exchange solution for an arbitrary, coplanar initial trajectory.

ball from point P to mouth 2, then through the wormhole in accord with the wormhole-traversal rule, then back to point P. That the trial and error will produce precisely one path of the desired type is demonstrated by the sequence of trials β, γ, $\delta, \ldots,$ ι. The wormhole traversal rule (2.1b) guarantees that the modest displacements of the path into mouth 2, in going from β to γ to ... to ι, will produce the large swing of the path around mouth 1 that is shown in Fig. 8. This large swing, in fact, is an obvious consequence of the "diverging-lens" property of any wormhole mouth [13,1]. And this monotonic, "diverging-lens swing" will obviously produce precisely one path of the desired form: path δ in Fig. 8. (iii) From the collision-to-collision travel distance along path δ and the backward time travel $T_d = 1$ of the wormhole traversal, compute the speed $v_2 = v_1'$ with which δ must be traversed. This, together with the path δ, gives the velocities $\mathbf{v}_2$ and $\mathbf{v}_1'$. (iv) From the fact that these $\mathbf{v}_2$ and $\mathbf{v}_1'$ must be the reflection of each other in the mirror line, infer the mirror line's orientation. (v) From the fact that the mirror line must be parallel to $\mathbf{v}_1 + \mathbf{v}_2$, and from the known value of $\mathbf{v}_2$ and direction of $\mathbf{v}_1$ (along α), *compute the ball's initial speed* v_1. (vi) From the initial speed and direction infer the initial velocity $\mathbf{v}_1$. (vii) Reflect this $\mathbf{v}_1$ in the mirror line to get $\mathbf{v}_2'$. All details of the solution are now known, and all the ball's equations of motion have been satisfied.

This same method can be used to produce solutions with one mirror-exchange collision and an arbitrary number of wormhole traversals:

For simplicity, restrict attention to a ball with radius R and a wormhole with mouth separation $D \equiv 1$ and mouth radius B satisfying

$$R \ll B \ll 1 \ . \tag{3.3}$$

Consider an arbitrary coplanar initial trajectory, as shown in Fig. 9(a). It is characterized by the ball's initial speed v_1, the angle ψ_A that its initial velocity makes with the mouths' line of centers, and its initial impact parameter h with respect to the center of mouth 2. (The subscript A is used on ψ_A because, in the limit that the collision point is infinitely far from the wormhole, the angle ψ_0, at which the ball first hits mouth 2, asymptotically approaches ψ_A; cf. Eq. (3.10) below: ψ_A is the *asymptotic* value of ψ_0.) By suitable choices of these parameters in the range $0 \le v_1 < \infty$, $0 \le \psi_A \le \pi$, and $-\infty < h < \infty$, we can describe all possible coplanar initial trajectories. (Trajectories with $-\pi < \psi_A < 0$ are obtained from those with $0 < \psi_A < \pi$ by reflection in the line of centers.) As we shall see, to obtain an infinite number of solutions, each with a single mirror-exchange collision and all with the same initial trajectory, we need only place two constraints on the initial trajectory:

$$v_1 > 1, \quad \psi_A > B \ . \tag{3.4}$$

There typically will be solutions (e.g., the class-I and class-II solutions of Fig. 3) in which the collision occurs in the vicinity of the wormhole. However, in this section, in order to demonstrate the existence of infinite numbers of solutions, we can and shall restrict attention to collisions that occur far from the wormhole, i.e., at

$$L \gg 1 \quad \text{and} \quad L \gg h \ , \tag{3.5}$$

where L is the distance, along the initial trajectory, from the collision to the point of closest approach to mouth 2; cf. Fig. 9(a). As was the case in Fig. 7, for a fixed incoming trajectory, the location L of the collision will turn out to depend on the number n of wormhole traversals, and in the limit $n \to \infty$, L will become arbitrarily large. In the discussion associated with Fig. 8, we regarded the initial path and L as fixed, and solved for the initial speed v_1. Here we shall regard the initial path and speed (i.e., ψ_A, h, and v_1) as fixed and shall solve for L in terms of ψ_A, h, v_1, and n.

Because $L \gg 1$, the velocity $\mathbf{v}_1'$ with which the ball

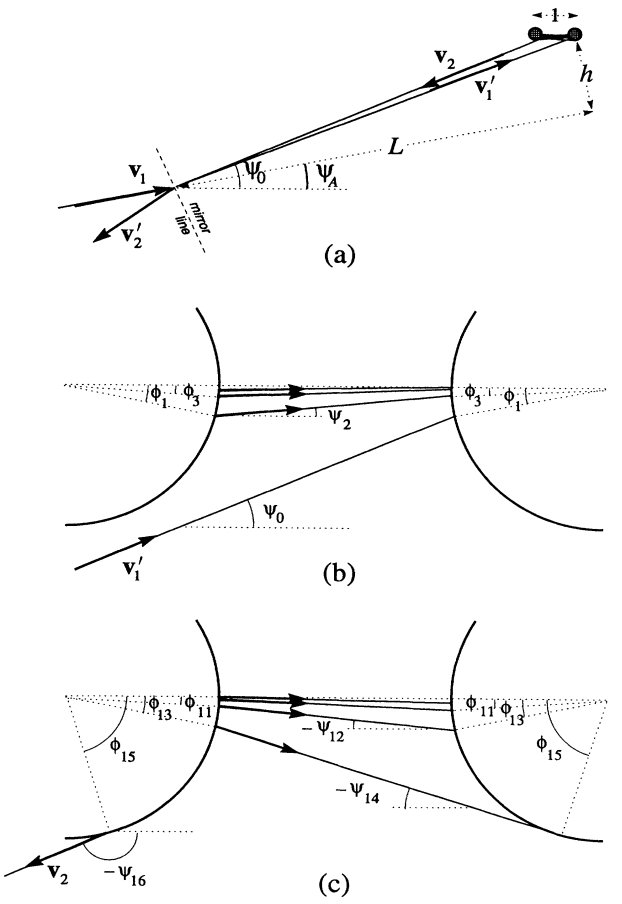

FIG. 9. A solution to the equations of motion for $R \ll B \ll 1$, with an arbitrary number n of wormhole traversals. The figure is drawn for $n = 8$. The initial trajectory, characterized by v_1, ψ_A, and h, is arbitrary except that $v_1 > 1$ and $\psi_A > B$. (a) The large-scale geometry of the solution. (b) The sequence of wormhole traversals as the ball works its way up toward the line of centers. (c) The sequence of traversals as the ball works its way back down from the line of centers. The angles ψ_{2k} and ϕ_{2k+1} are given by the diverging-lens map (3.6).

heads toward the wormhole and the velocity $\mathbf{v}_2$ with which it returns are very nearly antiparallel. Since these velocities must be the reflections of each other, the mirror line (which is along $\mathbf{v}_1 + \mathbf{v}_2$) must be very nearly orthogonal to $\mathbf{v}_2$, and correspondingly, the speeds must be related by

$$v_2 = v_1' = v_1 \cos(h/L) = v_1[1 - \tfrac{1}{2}(h/L)^2] , \qquad (3.6)$$

where we ignore corrections of higher order in h/L. In its sequence of n wormhole traversals, the ball goes backward in time by $\Delta T = -nT_d = -n$. Correspondingly, in order to return to the collision point at the moment of collision, it must travel a total distance nv_2. The total distance traveled, for large L and n, is easily seen from the diagram to be $2L + n$ (aside from unimportant fractional corrections of order h^2/L^2). By equating these distances to each other and using the value (3.6) for the speed v_2, we obtain the relation

$$n = \frac{2L}{v_1 - 1 - \frac{1}{2}(h/L)^2 v_1} . \qquad (3.7)$$

This is the promised relation which determines the location L of the collision in terms of the initial trajectory (characterized here by h and v_1) and the number n of wormhole traversals.

Notice that this relation cannot be satisfied, for arbitrarily large n and positive L, unless $v_1 > 1$. This is the origin of the first of constraints (3.4) on our initial trajectory. The second of those constraints, $\psi_A > B$, is required to ensure that, for arbitrarily large L and n [which means for $\psi_A \simeq \psi_0 \simeq 2\phi_1$ in Fig. 9(b), see discussion below], the ball can reach mouth 2 on its after-collision inward trajectory, without first running into mouth 1.

For a wide class of initial trajectories, there is a lower bound on the number n of wormhole traversals that can produce a self-consistent solution. In the regime of our analysis ($n \gg 1$, $L \gg 1$, $L \gg h$) this lower bound shows up as the fact that n viewed as a function of L with fixed v_1 and h [Eq. (3.7)] has a minimum:

$$n_{\min} = \frac{3\sqrt{3v_1/2}}{(v_1 - 1)^{3/2}} |h| . \qquad (3.8)$$

As the initial speed v_1 decreases toward unity (with h fixed), the minimum number of traversals $n_{\min}$ increases toward infinity.

To recapitulate, for every choice of initial conditions in the range $v_1 > 1$ and $\psi_A > B$, there is an infinite number of solutions (labeled by n) to (i) the laws of energy and momentum conservation in the billiard-ball collision [embodied in Eq. (3.6) which produces mirror-exchange], and (ii) the condition that the ball return to its collision point at the same time T as it left it [Eq. (3.7)]. We can be sure that each $n > n_{\min}$ gives a full solution to the equations of motion as soon as we have verified one more thing: that there is a path leading from the collision point of Fig. 9(a), to mouth 2, then through the wormhole n times [*and obeying the rules* (2.1) *at each traversal*], then out of mouth 1 and back to the collision point. We shall now demonstrate that this is so.

We shall label the wormhole traversals by odd integers $1, 3, 5, \ldots, 2n - 1$, and shall label the path up to mouth 2, the paths between traversals, and the path back to the collision point by even integers $0, 2, 4, \ldots, 2n$. Figure 9 is drawn for $n = 8$, $2n = 16$. The location of traversal $2k - 1$ is described by its angle ϕ_{2k-1} on the wormhole mouths relative to the line of centers, and the direction of path $2k$ is described by the angle ψ_{2k} from the line of centers to the path's velocity direction. The wormhole traversal rule (2.1b), in this notation, reads

$$\psi_{2k+2} - \psi_{2k} = -2\phi_{2k+1} \quad \text{for } 0 \le k \le n - 1; \qquad (3.9a)$$

and the expression for the slope of path $2k$ in terms of the locations of its end points reads (for $B \ll 1$ so $|\psi_{2k}| \ll 1$)

$$\sin\phi_{2k+1} - \sin\phi_{2k-1} = -\frac{\psi_{2k}}{B} \text{ for } 1 \le k \le n - 1 . \qquad (3.9b)$$

For all except the first and last traversals, the angle ϕ is small compared to unity. Therefore, in (3.9b) *the* $\sin\phi_{2k\pm1}$ *can be approximated by* $\phi_{2k\pm1}$, *except for* $\sin\phi_1$ *and* $\sin\phi_{2n-1}$.

Equations (3.9a) and (3.9b) constitute a map from the direction ψ_0 of the ingoing path to the direction ψ_{2n} of the outgoing path. This map embodies all the equations-of-motion constraints on the trial-and-error search for the desired ingoing path. In this map we are to take ψ_0 as fixed by our chosen location for the collision

$$\psi_0 = \psi_A + h/L \qquad (3.10)$$

[cf. Fig. 9(a)], and we are to adjust the location ϕ_1 of the ingoing path so as to produce n wormhole traversals followed by an outgoing path with direction $\psi_{2n} = \psi_0 - \pi$. The diverging-lens behavior of the wormhole guarantees that ϕ_1 can be so adjusted: By elementary geometric optics it should be clear that the correct route must work its way up toward the mouths' line of centers in the manner of Fig. 9(b) during the first half of its trip, and must then work its way back down in the manner of Fig. 9(c) during the second half. In order to do this successfully, the paths on the upward route must have $\psi_{2k+2} \ll \psi_{2k}$ and, correspondingly [cf. Eq. (3.9a)], $\phi_{2k+1} \simeq 2\psi_{2k}$—or, as one sees from a more precise study of the map (3.9a) and (3.9b), $\phi_{2k+1} = 2\psi_{2k}[1 + O(B)]$, where $O(B)$ denotes a k-dependent quantity of order B. In particular (choosing $k = 0$), ϕ_1 must be equal to $\frac{1}{2}\psi_0[1 + O(B)]$.

We can understand qualitatively (but not quantitatively), with the aid of Fig. 8, how the pattern of paths in the vicinity of the hole changes as the trial-and-error value of ϕ_1 is gradually decreased toward and then past the fixed $\frac{1}{2}\psi_0$. Initially, for $\phi_1 \simeq \pi/2$, there is just one wormhole traversal and the outgoing path at mouth 1 has the form β of Fig. 8. As ϕ_1 is decreased, the outgoing path at mouth 1 swings from β to γ, which is the desired path in our present trial-and-error search [point P very far down path γ as in Fig. 9(a)]. We thereby obtain a solution with one wormhole traversal. As ϕ_1 is further decreased, the output path at mouth 1 swings through δ and ε and up to ζ. Suddenly at ζ the output path plunges down mouth 2 and emerges from mouth 1

along β. A further decrease of ϕ_1 swings the output path around to γ, the desired position. We now have a solution with two wormhole traversals. By continuing to decrease the trial-and-error ϕ_1 toward $2\psi_0$, we cause the output path to swing again from γ to ζ, there enter the wormhole a second time and emerge on β, then swing down to γ, producing a solution with three traversals, then continue its swing to produce solutions with four traversals, five traversals, six traversals, ... Ultimately, as ϕ_1 decreases through the singular limit point of an infinite number of traversals [ϕ_1 = a certain value $\phi_{1\text{crit}} = \frac{1}{2}\psi_0 + O(\psi_0 B)$], the output path flips over to path η, which passes just above mouth 2; and further decreases of ϕ_1 cause it to swing through a pattern η, θ, ι, reduction of traversals by 1; then η, θ, ι, reduction by 1; ... until the number of traversals is reduced to zero. During this reduction sequence we get no acceptable solutions because the output path is not swinging through the required position γ.

This completes our demonstration that for each coplanar initial trajectory with $v_1 > 1$ and $\psi_A > B$ (and for a ball and wormhole satisfying $R \ll B \ll 1$), there exists an infinite number of solutions of the billiard-ball equations of motion, one corresponding to each value $n > n_{\min}$ of the number of wormhole traversals. To construct the solution with n traversals one can (i) specify the initial trajectory (the parameters ψ_A, h, v_1), (ii) then compute the location L of the collision from Eq. (3.7), and (iii) then find the location ϕ_1 at which the ball first enters mouth 2 by the above geometrical trial-and-error method. (Readers who seek higher rigor than we do might worry that our analysis has examined only the leading-order effects in the small parameters B, R/B, $1/L$, and h/L and has not proved rigorously that higher-order corrections are negligible. We are not worried.)

C. Initial trajectories with only one solution

In this section we turn attention from initial trajectories with infinite multiplicity (an infinite number of solutions), to the issue of whether there exist trajectories with only one solution: collision-free motion. As in the last section, we shall restrict attention to initial trajectories that are coplanar with the wormhole's line of centers and shall describe them by the parameters v_1, h, and ψ_A of Fig. 9(a).

We learned in the last section that for speeds $v_1 > 1$ the multiplicity is almost always infinite. This suggests that we should seek unit multiplicity in the regime $v_1 \ll 1$. Moreover, it seems intuitively clear that a good strategy for avoiding collisions is to keep the initial trajectory far from the wormhole, i.e., to choose $h \gg 1$.

That $h \gg 1$ and $v_1 \ll 1$ are indeed likely to produce unit multiplicity we can see from the following: If there were a solution with one or more collisions, the first collision encountered by the ball presumably would have to be of the type depicted in Fig. 9(a): the old incarnation of the ball flies out from near the wormhole and knocks the young incarnation inward, toward it, and then the old incarnation flies away never to collide again. Such a collision can only be of the mirror-exchange type and not the velocity-exchange type. Moreover, even if the ball encounters many additional collisions near the wormhole, energy conservation in the entire sequence of collisions implies that $v_2 = v_1'$ in the ball's first, distant collision; and this, together with the argument preceding Eq. (3.6), implies that

$$v_2 = v_1' = v_1 \cos(\psi_0 - \psi_A) < v_1 \ll 1 \ . \tag{3.11}$$

In other words, after its first collision, the ball heads toward the wormhole with a speed $v_1' = v_2$ very small compared to $D/T_d = 1$, and after it has finished all its near-wormhole activity, it heads back out toward its first collision with the same tiny speed. This implies, in turn, that the ball must travel backward in time, via wormhole traversals, by a huge amount, $\Delta T > 2h/v_2 > 2h/v_1 \gg 2h \gg 1$. Since each traversal produces a backward time travel of only $T_d = 1$, and there is a forward time travel of at least $D/v = 1/v$ between traversals, the only way the ball can achieve such an evolution is by a peculiar sequence of multiple collisions near the wormhole that build up speeds $v > 1$, temporarily, followed (from the ball's viewpoint) by multiple wormhole traversals into the past at these high speeds, and then followed (from the ball's viewpoint) by collisions that reduce the ball back to $v_2 \ll 1$ and send it back out toward its first collision event. We have searched cursorily for such peculiar solutions, without success, and we suspect they do not exist. However, we have no proof.

On the other hand, in the limit that the ball's initial velocity is precisely zero, and the ball's initial location is far from the wormhole mouths, it is easy to prove (with one caveat; see below) that there is only one solution, the trivial one where the ball remains always at rest. The proof makes use of a sequence of nested convex surfaces that enclose the wormhole mouths, which for concreteness we take to be ellipsoids of revolution (Fig. 10). The ellipsoids are labeled by a generalized radius r which increases outward. We require that the ball initially reside at a radius r_0 larger than that, $r_{\min}$, of the ellipsoid which barely encloses both wormhole mouths.

Now, suppose that there were a solution to the equations of motion other than the one in which the ball re-

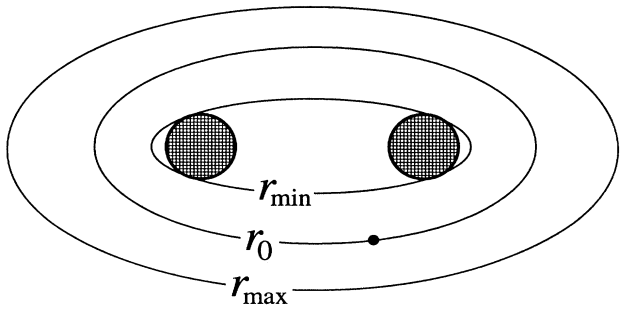

FIG. 10. Nested ellipsoids of revolution surrounding the wormhole, which are used to prove that a ball initially at rest sufficiently far from the wormhole must always remain at rest.

mains at rest. In this solution, the ball would have to undergo one or more self-collisions. There are two possibilities: (i) As seen by the ball there is an infinite sequence of self-collisions that goes on and on forever. We have not been able to rule out such a solution rigorously, but it seems exceedingly unlikely that one could exist. (ii) As seen by the ball there is a last collision. We restrict ourselves to this case.

After completing all its collisions, in order to conserve energy (cf. Fig. 5 of Ref. [6]), the ball would have to return to rest. Let $r_{\max}$ be the largest radius the ball reaches while it is in motion. Since $r_{\max} \geq r_0 > r_{\min}$, this largest radius must lie outside the wormhole, and there thus must be a collision at this $r_{\max}$, for otherwise the moving ball would be at larger radii momentarily before or after it is at $r_{\max}$. However, the object that the ball collides with, as it rises to $r_{\max}$ and then gets deflected back downward, can only be the ball itself (since there exist no objects in this problem except the ball and the wormhole), on a path that is coming downward from radii $r > r_{\max}$. We thus reach a contradiction; $r_{\max}$ is not the ball's maxium radius. Therefore, there exist no solutions except the trivial one.

Note that this proof fails if the ball is initially at rest inside radius $r_{\min}$, since the maximum radius then can lie at the wormhole mouth, and the wormhole rather than a collision can be responsible for deflecting the ball back inward toward smaller radii. A specific example of a nontrivial solution of this type is the one where the ball is initially at rest on the mouths' line of centers, gets hit and knocked into mouth 2, emerges earlier from mouth 1, hits itself and returns to rest; cf. the second paragraph after Eq. (3.1).

IV. SEARCH FOR COPLANAR INITIAL TRAJECTORIES WITH NO SELF-CONSISTENT SOLUTIONS

We now turn attention to the issue of whether there exist coplanar initial trajectories with vanishing multiplicity—i.e., initial trajectories that have no self-consistent solutions whatsoever. If there are such initial trajectories, they must be of the "dangerous" type, i.e. they must be trajectories that, when followed assuming no self-collision, produce a self-collision; cf. the discussion in Sec. I B.

Our search for zero multiplicity among the dangerous trajectories will be carried out in three pieces. In subsection A we shall consider the restrictive case of a ball and wormhole satisfying $R \ll B \ll 1$, and shall show that in this case all (coplanar) dangerous initial trajectories have infinite multiplicity. In Sec. IV B and Appendix A, we shall completely relax these restrictions, and require only that $B < \frac{1}{2}$ so the wormhole mouths do not overlap each other, and $R/B < \frac{1}{2}$ so the ball can pass through the wormhole and we can ignore the effects of tidal forces on the ball during and after its traversal (cf. Sec. II A). For this case we shall derive a pair of coupled, highly nonlinear algebraic equations that govern self-consistent solutions. These equations have solutions in all regimes we have examined (the multiplicity is nonzero), but their high nonlinearity has prevented us from proving definitively that there always is a solution. In Sec. IV C and Appendix B we shall examine the intermediate case $R/B < \frac{1}{2}$ but $B \ll 1$. In this case we shall show that for a wide range of dangerous initial trajectories there is always at least one self-consistent solution, and we shall argue that this is probably so for all initial trajectories, i.e., the multiplicity is probably always nonzero.

To summarize, our search will turn up no evidence at all for initial trajectories with zero multiplicty.

As a by-product of our search, we shall obtain a detailed understanding of the class-I and class-II solutions depicted in Fig. 3, above.

A. Ball and wormhole with $R \ll B \ll 1$

When $R \ll B \ll 1$, we can infer from the analysis given in Sec. III B above that all dangerous initial trajectories have infinite multiplicity. The argument goes as follows.

Each dangerous initial trajectory, if followed assuming no self-collision, must travel backward in time by a mouth-2 to mouth-1 wormhole traversal so as to produce a self-collision. This means that it must hit mouth 2 upon nearing the wormhole, and not be blocked from doing so by mouth 1, which in turn means that the angle ψ_A in Fig. 9(a) must be larger than B:

$$\psi_A > B \tag{4.1a}$$

[cf. Eq. (4.7) below with $\psi_A = \theta + \phi$]. Moreover, it is easy to see that, if n is the total number of mouth-2 to mouth-1 wormhole traversals that the (self-inconsistent) trajectory undergoes before hitting itself, then the total distance it travels from its first encounter with the event of self-inconsistent collision to its second encounter is $\Delta l > nD = n$. Since the wormhole traversals produce a backward time travel of $\Delta T = -nT_d = -n$, the demand that there be zero external time lapse between the first and second encounters, $\Delta l/v_1 + \Delta T = 0$, implies that the ball's initial speed is

$$v_1 > 1 \ . \tag{4.1b}$$

Since each dangerous initial trajectory satisfies conditions (4.1a) and (4.1b), all dangerous initial trajectories are in the class for which we proved infinite multiplicity in Sec. III B; cf. Eq. (3.4).

B. $B < \frac{1}{2}$ and $R/B < \frac{1}{2}$

Turn next to a wormhole whose size is constrained only by $B < \frac{1}{2}$ (mouths do not overlap) and $R/B < \frac{1}{2}$ (tidal forces ignorable during traversal; cf. Sec. II A).

As in the extreme case of $R \ll B \ll 1$, so also here, all dangerous initial trajectories must extend directly from infinity to mouth 2, so as to initiate their backward time travel. This makes it advantageous to label the initial trajectories by a different triplet of parameters than those of Fig. 9(a) above. The previous parameters were the

initial speed v_1 of the ball's center, its impact parameter h, and its angle ψ_A relative to the wormhole mouths' line of centers. Our new parameters are v_1 and the two angles θ, ϕ shown in Fig. 11. The two sets of parameters are related by $h = -B\sin\theta$, $\psi_A = \theta + \phi$.

In order to make progress in the search for self-consistent solutions in this weakly constrained case of possibly large B and R/B, we have confined our search to self-consistent solutions (i) with just one collision, which (ii) is of the mirror-exchange type, and (iii) in which the ball first encounters the collision event before any wormhole traversal and then encounters it again after only one traversal. We shall characterize such a self-consistent solution by (among others) the two angles α and β shown in Fig. 11; β is the ball's deflection angle when it first passes through the collision event, and α is the angle between the two incoming balls (old incarnation and new incarnation) at the collision event. In Appendix A we show that, corresponding to each nonspurious solution (α, β) of the following two equations, there exists a self-consistent solution of the full equations of motion for the billiard ball; and we give in Appendix A equations for computing all features of that solution. The two equations for α and β are

$$B\sin\alpha\sin\frac{\alpha-\beta}{2}\left[\sin\theta-\sin\left(\theta+\phi-\frac{\alpha-\beta}{2}\right)\right]$$

$$+\sin\beta\sin\frac{\alpha-\beta}{2}\left\{\sin(\theta+\phi)-B\left[\sin\theta+\sin\left(\theta+\phi+\frac{\alpha-\beta}{2}\right)\right]\right\}=(v_1+d)\sin\frac{\alpha+\beta}{2}\sin\alpha\sin\beta\ , \quad (4.2)$$

$$B\sin\left(\frac{\alpha+\beta}{2}-\theta-\phi\right)(\sin\alpha+\sin\beta)+B\sin\theta\sin(\alpha-\beta)-\sin\beta\sin(\alpha-\theta-\phi)=-d\sin\alpha\sin\beta, \quad (4.3)$$

where

$$\rho=\frac{\sin[\frac{1}{2}(\alpha+\beta)]}{\sin[\frac{1}{2}(\alpha-\beta)]}\ , \quad (4.4a)$$

$$d=2sR/(1+\rho^2+2\rho\cos\alpha)^{1/2},\quad s=\mathrm{sign}(d)\ ; \quad (4.4b)$$

and if one is interested in the ball's speed between collisions, it is given by

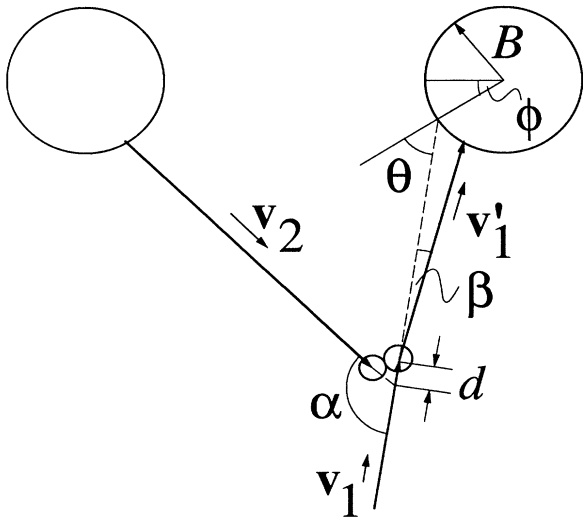

FIG. 11. Geometry of a self-consistent solution with one wormhole traversal and one billiard-ball collision. More details of this geometry are depicted in Figs. 17 and 18 of Appendix A. By convention all angles and distances (e.g., α, β, and d) are positive when their orientations are as shown here.

$$v_2=v_1\rho\ . \quad (4.5)$$

The parameter d is shown in Fig. 11; it is the distance that the ball's younger incarnation must travel *past* the point of intersection of the two incoming trajectories, to reach the collision event. One can choose its sign s arbitrarily in a search for solutions. If $s=+1$ (the case shown in Fig. 11), the ball's older incarnation passes behind the younger, the younger is deflected to the right ($\beta>0$), and we call the collision "class I" [cf. Fig. 3(b)]. If $s=-1$, the older incarnation passes in front of the younger, the younger is deflected to the left ($\beta<0$), and we call the collision "class II" [cf. Fig. 3(c)]

Equations (4.2) and (4.3) for α and β have the following set of *spurious solutions* that were introduced by manipulations carried out in Appendix A:

$$(\alpha,\beta)=(0,0),\ (\pi,0),\ (0,\pi),\ (\pi,\pi),\ (2\phi,0)\ , \quad (4.6a)$$

$$\text{any solution with } \rho<0\ , \quad (4.6b)$$

$$\text{any solution with } \mathrm{sign}(\beta)\neq\mathrm{sign}(d)\equiv s\ . \quad (4.6c)$$

Equations (4.2) and (4.3) for α and β are so horribly nonlinear that we can say only one thing definitive and universal about their solutions: since there are two equations for two unknowns, the solutions must form a discrete set. It is far from obvious, just looking at the equations, whether there exist values of the wormhole and ball radii B, R and initial-trajectory parameters v_1, θ, ϕ that produce zero solutions. Numerical exploration, and the analytic considerations of the next section, have not turned up any such zero-multiplicity trajectories.

C. $B \ll 1$ and $R/B < \frac{1}{2}$

To make further progress in our search for dangerous initial trajectories with no self-consistent solutions, we shall retain $R/B < \frac{1}{2}$, but shall specialize to a wormhole with mouth radii small compared to their separation, $B \ll D = 1$. (Note that these relations imply $R \ll 1$.) We shall also limit ourselves to a large but not complete set of dangerous initial trajectories: those whose self-*inconsistent* solutions have the same form as the self-consistent solutions analyzed in the last section: the ball comes in from infinity, passes through (and ignores) its collision event, traverses the wormhole just once, and then hits its collision event a second (self-inconsistent) time. The parameters of such initial trajectories lie in the range

$$B/2 < \phi < \pi/2, \quad B - \phi < \theta < \phi, \quad v_{1\min} < v_1 < v_{1\max} , \tag{4.7}$$

where

$$\left.\begin{matrix} v_{1\min} \\ v_{1\max} \end{matrix}\right\} = \frac{\cos\theta}{\cos\phi}(1 - 2B\cos\phi) \mp \frac{2R}{\cos\phi} . \tag{4.8}$$

The θ, ϕ part of this dangerous region is the interior of the thick-lined triangle of Fig. 12. We shall call this the "dangerous triangle." The constraint $\theta > B - \phi$ (lower left edge of dangerous triangle) is required so the ball will avoid entering mouth 1 before it reaches mouth 2; parameters (θ, ϕ) near this edge correspond to incoming trajectories that skim past mouth 1, go down mouth 2, emerge from mouth 1, and then collide self-inconsistently near mouth 1. The constraint $\phi < \pi/2$ (right edge of dangerous triangle) is required so the ball's path will intersect itself after passing through the wormhole; near this edge the outgoing path emerges from the wormhole nearly antiparallel to the ingoing path, thereby producing a self-inconsistent collision far from the wormhole. The constraint $\theta < \phi$ (upper left edge of dangerous triangle) is required to make the collision occur before the ball enters mouth 2 a second time; for (θ, ϕ) near this edge, the self-inconsistent collision occurs close to mouth 2. The constraint (4.8) on v_1 (not depicted in the figure) guarantees that the ball returns to the collision region at the right time to produce a self-inconsistent collision.

In Appendix B we carry out a search for self-consistent solutions throughout this range of dangerous initial trajectories. The strategy of the search is based on the physical idea that, because $R < B/2 \ll 1$, the ball travels a distance huge compared to its size R between its first and second encounters with the collision. This means that a very tiny deflection, $|\beta| \sim R \ll 1$, can significantly alter the geometry of the collision, and possibly change it from the self-inconsistent form of Fig. 3(a) to the class-I or class-II self-consistent form of Figs. 3(b) and 3(c). A tiny value of $|\beta|$ goes hand in hand with a tiny change of α from its self-inconsistent-solution value 2ϕ (which is dictated by the wormhole traversal rule shown in Fig. 4). This motivates us to search for solutions in the parameter range

$$|\beta| \ll 1, \quad |\varepsilon| \ll 1 , \quad \text{where } \varepsilon \equiv \alpha - 2\phi . \tag{4.9}$$

In Appendix B we search in this range by expanding Eqs. (4.2) and (4.3) for α, β in powers of ε and β. In order to obtain real solutions, rather than just the spurious solutions of Eq. (4.6a), the equations are expanded to quadratic order, and they then are combined to yield one quadratic and one linear equation, Eqs. (B2) and (B12) [in which λ_1 is as defined in Eq. (4.10) below]. These equations have simple analytic solutions throughout the regime (4.7) of dangerous initial trajectories (throughout the interior of Fig. 12's dangerous triangle), except near the triangle's left corner and near its lower left edge.

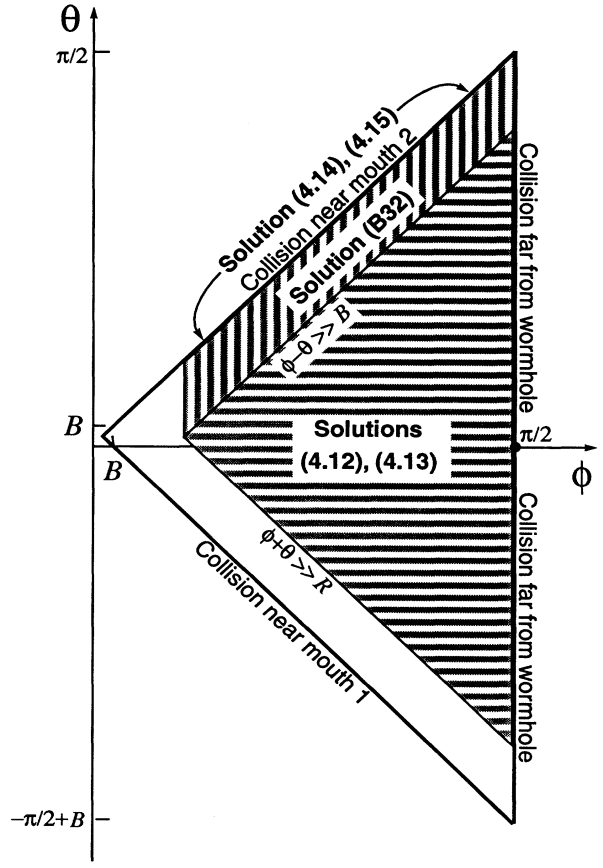

FIG. 12. Parameter space for the ball's initial trajectory when $B \ll 1$, $R/B < \frac{1}{2}$. The interior of the thick-lined triangle is the region of dangerous initial trajectories that produce a self-inconsistent collision after one wormhole traversal [Eq. (4.7)]. We call this the "dangerous triangle." Equations (4.2) and (4.3) govern solutions throughout this dangerous triangle. Simple analytic solutions of these equations are given, in the indicated shaded regions of the dangerous triangle, by the indicated equations. Analytic solutions cannot be derived by the techniques of Appendix B for the white regions of the triangle (left corner and lower left edge), but numerical solutions have been found in spot checks throughout that white region. Figure 14 below shows, as an example, a solution (part analytic, part numerical) all along the upper left edge of the dangerous triangle, including the left corner.

Near this corner and edge, tiny changes of the incoming trajectory produce huge changes in the location of the self-inconsistent solution; and correspondingly, it turns out that self-consistent solutions there typically have a large value of ϵ. This causes the power-series expansion of Appendix B to break down. However, near this corner and edge one can go back to the exact, nonlinear equations (4.2) and (4.3), and find solutions numerically. At all points near the left corner and lower left edge where we have tried, we found numerical solutions. Thus, it seems likely that solutions exist everywhere in the dangerous triangle.

The simple analytic solutions in the horizontally shaded central part of the triangle (i.e., for collisions not close to either mouth; cf. Fig. 12) are interesting and instructive. In describing these simple solutions we shall give formulas not only for β and ε (a surrogate for the angle α), but also for the ball's speed v_2 between collisions. Other parameters describing the solutions can be inferred from the equations in Appendix A. To simplify notation in the solutions, we shall characterize the initial speed v_1 and the speed between collisions v_2 by parameters λ_1 and λ_2 defined by

$$v_1 = v_{1\min} + \lambda_1(v_{1\max} - v_{1\min}) , \tag{4.10}$$

$$v_2 = v_{1\min} + \lambda_2(v_{1\max} - v_{1\min}) . \tag{4.11}$$

Note that the dangerous initial trajectories have $0 < \lambda_1 < 1$. In the central region of the triangle ($\phi - \theta \gg B$, $\phi + \theta - B \gg R$, and $\pi/2 - \phi \gg B$) there are two simple solutions to the quadratic and linear equations (B2) and (B12): one of class I, the other of class II. The class-I solution ($s = +1$) is

$$\beta = \frac{8\sin\phi}{\cos\theta(\tan^2\phi - \tan^2\theta)} BR\lambda_1 , \tag{4.12a}$$

$$\varepsilon = \frac{8\cos\phi}{\sin(\theta+\phi)}\lambda_1 R , \tag{4.12b}$$

$$\lambda_2 = \left(1 + \frac{2\cos\phi}{\tan^2\phi - \tan^2\theta} B\right)\lambda_1 . \tag{4.12c}$$

The class-II solution ($s = -1$) is

$$\beta = -\frac{8\sin\phi}{\cos\theta(\tan^2\phi - \tan^2\theta)} BR(1-\lambda_1) , \tag{4.13a}$$

$$\varepsilon = -\frac{8\cos\phi}{\sin(\theta+\phi)}(1-\lambda_1)R , \tag{4.13b}$$

$$1 - \lambda_2 = \left(1 + \frac{2\cos\phi}{\tan^2\phi - \tan^2\theta} B\right)(1-\lambda_1) . \tag{4.13c}$$

These solutions, which when viewed as functions of λ_1 (i.e., of v_1) are linear, actually extend out of the region $0 < \lambda_1 < 1$ of dangerous initial trajectories: The class-I solution is valid for $R^{-1} \gg \lambda_1 > 1$, as well as for $0 < \lambda_1 < 1$, but it is spurious for $\lambda_1 < 0$ since there it predicts opposite signs for β and s; cf. Eqs. (4.12a) and (4.6c). Similarly, the class-II solution is valid for $-R^{-1} \ll \lambda_1 < 0$, as well as for $0 < \lambda_1 < 1$, but for $\lambda_1 > 1$ it predicts opposite signs for β and s and thus is spurious. At the point $\lambda_1 = 0$ or 1 where one of the solutions stops (becomes spurious), it actually joins onto (converts over into) a valid, collision-free solution in a manner depicted in Fig. 13.

These simple solutions for the interior region of the dangerous triangle (Fig. 12) break down near the triangle's upper left and lower left edges. There, in solving the coupled linear and quadratic equations (B2) and (B12), one must keep nonlinear terms. It is straightforward to do so, and thereby obtain solutions valid near the upper left edge, but not near the left corner or lower left edge. In Appendix B we analyze the region near the upper left edge (collisions that occur near mouth 2): $0 < \phi - \theta \lesssim B$, $\phi \gg B$. By combining Eqs. (B2) and (B12), we obtain a quadratic equation [Eq. (B29)], with rather simple coefficients, for the incoming ball's deflection angle β. Some of the solutions to this quadratic equation are spurious (wrong sign of β for a chosen sign of s). In Appendix B it is shown that, throughout our chosen region ($0 < \phi - \theta \lesssim B$, $\phi \gg B$), there is a nonspurious class-I ($s = +1$) solution, Eq. (B32), but in some parts of that region there is no nonspurious class-II solution. We suspect, but have not proved, that the missing class-II solution actually exists, but the ball first encounters its collision shortly after passing through the wormhole, rather than before, and therefore this solution is beyond the domain of validity of our analysis.

On the upper left edge of the dangerous triangle (at $\phi = \theta$), the class-I solution (B32) has the form depicted in Fig. 14. This figure is drawn for $\lambda_1 = \frac{1}{2}$, $B = 10^{-2}$

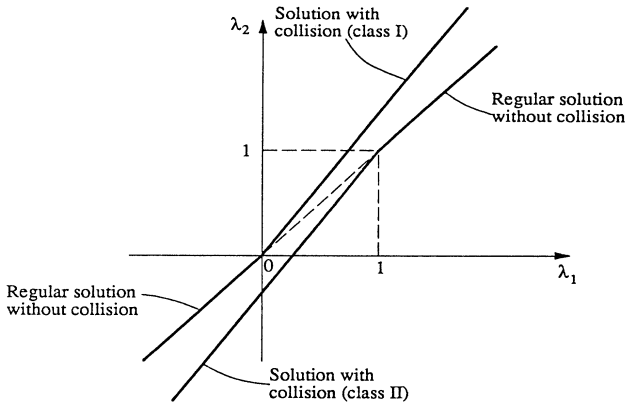

FIG. 13. Billiard-ball speeds for the two self-consistent solutions (4.12) and (4.13) in the central region of Fig. 12's dangerous triangle. (This central region represents collisions that occur neither very close to a wormhole mouth nor at huge distances from the wormhole.) The parameters plotted, λ_1 and λ_2, are proportional to the speeds v_1 and v_2 [Eqs. (4.10) and (4.11)], and the dangerous range of incoming speeds is $0 < \lambda_1 < 1$. At each edge of the dangerous range, one of the solutions joins continuously onto a collision-free solution, and the other continues to exist as a solution with collision.

and $R = 10^{-5}$ (though the solution is valid also when R is close to B). Notice the sharp change in the deflection angle as one passes from $\phi > \pi/4$ to $\phi < \pi/4$, and from $\phi > \sqrt{B} = 0.1$ to $\phi < \sqrt{B} = 0.1$: At $\phi > \pi/4$, the deflection angle β is of order $R = 10^{-5}$ [This is rather larger than in the central region of the triangle, where it is of order BR; cf. Eqs. (4.12a) and (4.13a)]. At $\sqrt{B} < \phi < \pi/4$, β is of order $B = 10^{-2}$. As ϕ decreases toward zero (as one moves toward the left corner of the dangerous triangle), ε grows large and the power series expansion of Appendix B begins to break down. We have solved numerically the full, nonlinear equations (4.2) and (4.3) for α and β in this corner region and have verified that a solution continues to exist right up to the corner.

The analytic solution (B32) takes on especially simple forms for a very small ball ($R\tan^2\phi \ll B$), very near the upper left edge of the dangerous triangle ($|\phi-\theta|\tan^2\phi \ll 1$), and away from the regions of rapidly changing β: At $\phi \gg \sqrt{B}$ and $\pi/4 - \phi \gg B$ the solution becomes

$$\beta = \sin\phi\cos 2\phi B, \quad \varepsilon = \frac{\cos 2\phi \cos^2\phi}{\sin\phi} B \ ; \tag{4.14}$$

and at $\phi - \pi/4 \gg B$ (but $\pi/2 - \phi \gg \sqrt{R/B}$ and $\pi/2 - \phi \gg |\phi - \theta|^{1/2}$), it becomes

$$\beta = \varepsilon = -\frac{4\sin\phi}{\cos 2\phi} R\lambda_1 \ . \tag{4.15}$$

These approximations to the solution are plotted as dashed lines in Fig. 14.

To recapitulate, self-consistent analytic solutions with $|\beta| \ll 1$ and $|\varepsilon| \ll 1$ exist throughout the dangerous region of Fig. 12, except its left corner and lower left edge; and we have found numerical solutions in spot checks of that corner and edge. We find no evidence, when $B \ll 1$ and $R/B < \frac{1}{2}$, for initial trajectories with zero multiplicity.

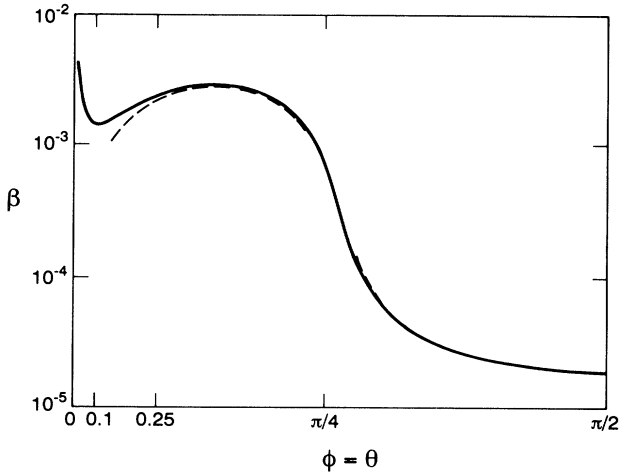

FIG. 14. A combination numerical and analytic solution for the ball's deflection angle β as a function of ϕ, along the upper edge $\theta = \phi$ of Fig. 12's dangerous triangle. This is the class-I solution ($\beta > 0$); the ball and wormhole radii are $R = 10^{-5}$ and $B = 10^{-2}$; and the incoming speed is at the center of the dangerous range, $v_1 = \frac{1}{2}(v_{1\max} + v_{1\min})$ [$\lambda_1 = \frac{1}{2}$; cf. Eq. (4.10)].

V. NONCOPLANAR TRAJECTORIES

In this section we shall extend most of the coplanar results of Secs. III and IV to initial trajectories that are slightly noncoplanar. Thereby we shall accumulate evidence which suggests, but does not really prove, that all noncoplanar initial trajectories have multiplicity larger than zero (i.e., have self-consistent solutions to the equations of motion). Throughout our discussion we shall confine attention to a wormhole with $B \ll 1$. [This same restriction was imposed throughout Sec. III and in all of Sec. IV except in the fully nonlinear equations of motion (4.2) and (4.3).]

As a first step, we shall ask ourselves how nearly coplanar a trajectory must be in order to be dangerous, i.e., in order to produce a self-inconsistent collision, if followed assuming no collision.

Consider an arbitrary initial trajectory. Define the wormhole's "equatorial plane" to be the unique plane that is parallel to this initial trajectory and contains the wormhole's line of centers. At any point along the ball's trajectory, denote by z the height of the ball's center above the equatorial plane, denote by l the distance the ball has traveled (from some arbitrary origin) parallel to the equatorial plane, and denote by $z' \equiv dz/dl$ the inclination of its trajectory to the equatorial plane. Our definition of equatorial plane guarantees that initially the trajectory has $z = \text{const} \equiv z_1$ and $z' = 0$. However, z' will be made nonzero by the first collision or wormhole traversal the ball encounters.

Now, follow the ball's initial trajectory assuming no collisions. In order for the trajectory to be dangerous, it must traverse the wormhole. The wormhole traversal will convert the trajectory's inclination from $z_1' = 0$ to $z_2' = \cos\theta\tan[2\arcsin(z_1/B)]$; cf. Fig. 15(a). Here θ is the angle at which the trajectory's equatorial projection intersects the equatorial normal to the wormhole mouth (as in Fig. 11 above). If it travels a subsequent distance $\Delta l = L_2$ parallel to the equatorial plane and then collides with itself (inconsistently), the height of its center at the collision will be $z_2 = z_1 + L_2\cos\theta\tan[2\arcsin(z_1/B)]$. To guarantee a collision, we must have $|z_2 - z_1| < 2R$. Thus, the initial trajectory will be *dangerous* only if

$$z_1 < B\sin[\tfrac{1}{2}\arctan(2R/L_2\cos\theta)] \ . \tag{5.1}$$

For typical dangerous initial trajectories, $L_2\cos\theta$ will be of order unity, and thus much larger than B, which in turn is a little larger than R; so the danger criterion (5.1) reduces to $z_1 \lesssim RB$. This means that the dangerous initial trajectories differ from coplanarity by no more than a fraction $B \ll 1$ of the ball's radius R.

We have not found a good way to analyze dangerous initial trajectories near the boundary of the region (5.1). However, for $z_1 \ll B\sin[\frac{1}{2}\arctan(2R/L_2\cos\theta)]$, the ball's motions parallel to the equatorial plane (its "in-plane motions") decouple from its motions perpendicular to the equatorial plane (its "out-of-plane motions"), and this

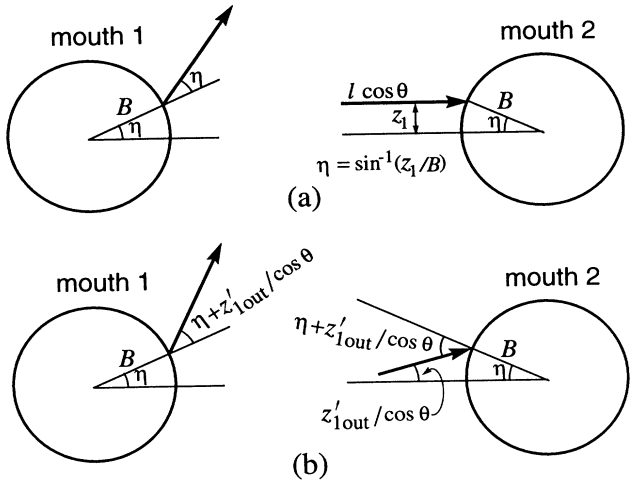

FIG. 15. Change in a noncoplanar trajectory's inclination z' when it traverses the wormhole from mouth 2 to mouth 1: (a) for a ball that does not collide before the traversal; (b) for a ball that collides and is vertically deflected before the traversal. (The change of inclination is a manifestation of the wormhole's "diverging-lens" effect.) The left and right halves of these two-dimensional diagrams are the projection of the ball's trajectory onto a plane that (i) is orthogonal to the equatorial plane (i.e., is vertical), and (ii) passes through the mouth's center and through the intersection of the trajectory with the mouth. The angle between the trajectory and this projection plane is θ, and correspondingly, horizontal distance along the projected trajectory is $l\cos\theta$.

permits us easily to extend to such trajectories most of the results of Secs. III and IV. We shall demonstrate this explicitly for self-consistent solutions that have just one wormhole traversal and one collision, and then shall argue that it is true also (though with a change in the allowed range of z_1) for all other self-consistent solutions.

Consider, then, a self-consistent solution in which the ball gets hit by itself, travels down mouth 2 and out of mouth 1, and then hits itself. We shall seek conditions on the degree of noncoplanarity that permit the in-plane motions to decouple from the out-of-plane motions.

Denote by z_1 and z_2 the out-of-plane displacements of the ball's younger and older incarnations at the moment of collision. Because the balls are round, the in-plane locations of the balls' centers are influenced by the out-of-plane displacements by amounts

$$\Delta l \sim R(1-\cos\psi) \simeq R\psi^2/2 \simeq \tfrac{1}{2}R[(z_2-z_1)/2R]^2 , \tag{5.2}$$

where ψ is the angle shown in Fig. 16. Similarly, if the ball's center passes through the wormhole mouths at a height $z_{\rm mouth}$, that height will influence the ball's in-plane motion in the same manner as would a decrease

$$\frac{\delta B}{B} \simeq -\frac{z_{\rm mouth}^2}{2B^2} \tag{5.3}$$

in the wormhole's radius. The back action of the out-of-plane motion on the in-plane motion will be negligible

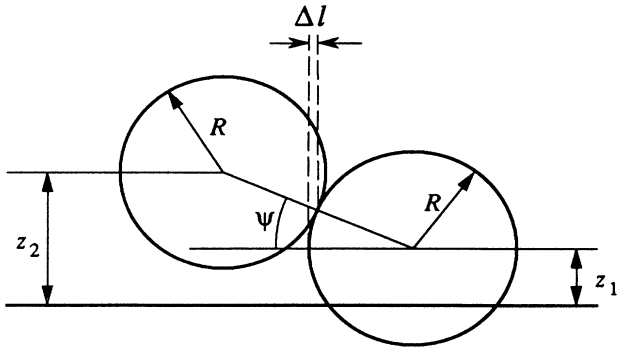

FIG. 16. Back action of a billiard ball's out-of plane motion on its in-plane motion.

in the collision and traversal if $\Delta l \ll R$ in (5.2) and $\delta B/B \ll 1$ in (5.3), i.e., if

$$|z_2 - z_1| \ll R \quad \text{and} \quad z_{\rm mouth} \ll B . \tag{5.4}$$

We now ask what values of z_1 lead to self-consistent solutions that satisfy this decoupling condition. [To keep formulas simple, we shall write them in approximate forms valid for the regime (5.4).]

In the collision, the z component of momentum transfer to ball 1 is

$$\Delta p_z = \frac{z_1 - z_2}{2R}\Delta p_l , \tag{5.5}$$

where $\Delta p_l = k m v_1 \beta$ (with k typically of order unity) is the momentum transfer in the plane, m is the mass of the ball, v_1 is the ball's speed before the collision, and β is the deflection angle in the plane. This z-momentum transfer changes the inclination of the ball's trajectory from $z'_{\rm 1in} = 0$ to

$$z'_{\rm 1out} = \frac{z_1 - z_2}{2R}\frac{\Delta p_l}{p_l} = \frac{z_1 - z_2}{2R}k\beta \ll 1 , \tag{5.6}$$

where $p_l = m v_1$ is the momentum in the plane. After traveling a distance L_1 from the collision point, the ball arrives at mouth 2 with height

$$z_{\rm mouth} = z_1 + z'_{\rm 1out}L_1 \ll B . \tag{5.7}$$

The wormhole's diverging-lens effect causes the ball to emerge from its traversal with inclination [Fig. 15(b)]

$$z'_2 = z'_{\rm 1out} + \frac{2z_{\rm mouth}\cos\theta}{B} \ll 1 . \tag{5.8}$$

The height z_2 that the ball reaches after traveling through the wormhole and returning to the collision point is

$$z_2 = z_{\rm mouth} + z'_2 L_2 . \tag{5.9}$$

Combining Eqs. (5.6), (5.7), (5.8), and (5.9), we obtain

$$z_2 - z_1 = \frac{(2L_2\cos\theta/B)z_1}{1 + (k\beta/2R)(L_1 + L_2 + 2L_1L_2\cos\theta/B)} , \tag{5.10a}$$

and correspondingly

$$z_{\text{mouth}} = \frac{[1+(k\beta/2R)(L_1+L_2)]z_1}{1+(k\beta/2R)(L_1+L_2+2L_1L_2\cos\theta/B)} . \tag{5.10b}$$

Note that, whatever may be the values of the parameters L_1, L_2, θ, and β, there always is a height z_1 that makes $z_2 - z_1$ and z_{mouth} small enough to satisfy the decoupling criteria (5.4). For the typical case of $\phi - \theta \gg B$, the distances of the collision from the mouths are $L_1 \sim L_2 \sim 1$ and the in-plane deflection angle in the collision is $\beta \sim BR$ [Eq. (4.12a)], so

$$z_2 - z_1 \sim z_1/B \quad \text{and} \quad z_{\text{mouth}} \sim z_1 , \tag{5.11}$$

and both decoupling criteria (5.4) are satisfied if

$$z_1 \ll BR . \tag{5.12}$$

Unfortunately (and not surprisingly), this decoupled range is a small portion of the full range of dangerous initial trajectories $z_1 < B\sin[\frac{1}{2}\arctan(2R/L_2\cos\theta)] \sim RB$. Thus, we can say nothing about the existence of solutions over the full range. However, in the decoupled range we can infer the following from the above analysis. (i) The in-plane motion is affected negligibly by the out-of-plane motion. (ii) If there exists a solution to the equations of motion for the in-plane motion, then there is also a solution for the out-of-plane motion, and it is described by the above equations. (iii) The in-plane motion is described by the same equations as for coplanar initial trajectories. (iv) Therefore, *to each solution for any slightly noncoplanar initial trajectory there corresponds a solution for the corresponding coplanar trajectory, and conversely.* We have derived this conclusion only for the case of solutions with a single collision and single wormhole traversal. However, it should be clear that the same method can be used to derive the same final conclusion for all self-consistent nearly coplanar solutions, regardless of the number of collisions and traversals. There will be a change in the precise criteria for decoupling of the in-plane motions from the out-of-plane motions, but there will always be some out-of-plane neighborhood of coplanar initial trajectories for which the conclusion holds true.

This implies that the results of Secs III and IV for coplanar trajectories are also valid for slightly noncoplanar trajectories. Specifically: (i) When $R \ll B \ll 1$ all initial trajectories have multiplicities greater than zero (i.e., have self-consistent solutions), and all dangerous initial trajectories have infinite multiplicity. (ii) When B is allowed to be of order unity (but no larger than $\frac{1}{2}$), and R/B is constrained only to be small enough to neglect tidal forces, the extensive set of dangerous initial trajectories investigated in Sec. IV and Appendix B all have self-consistent solutions even when they are perturbed slightly in a noncoplanar way.

To recapitulate, these conclusions hold only for a neighborhood of coplanarity (typically $z_1 \ll BR$) that is much smaller than the full range of dangerous initial trajectories (typically $z_1 \lesssim BR$). However, these conclusions make us suspect that even when $z_1 \sim BR$, all initial trajectories will have at least one self-consistent solution.

VI. CONCLUSIONS

We have found that the Cauchy problem for a billiard ball in a wormhole spacetime with closed timelike curves is ill posed in the sense that large, generic classes of initial trajectories have multiple, and even infinite numbers of self-consistent solutions to the equations of motion. On the other hand, we have seen no evidence for a stronger type of ill posedness: generic initial trajectories with no self-consistent solutions. In paper II [9] it will be shown that a sum-over-histories version of quantum mechanics restores well posedness to the Cauchy problem: Quantum mechanics predicts definite probabilities for a nearly classical billiard ball to follow this, that, or another of its classical solutions.

These results give a first glimpse of the behavior of interacting systems in wormhole spacetimes with closed timelike curves. It will be interesting to study more realistic, albeit more complex, classical and quantum systems, as some researchers are currently doing [10]. However, our results suggest that in general there might be no deep conflict between the existence of closed timelike curves and the standard laws of physics.

ACKNOWLEDGMENTS

We thank Joseph Polchinski for motivating this research by asking, in a letter to one of us, how the laws of physics could deal with paradoxical situations of the sort embodied in Fig. 3(a). For helpful discussions we thank John Friedman, Mike Morris, Nicolas Papastamatiou, Leonard Parker, and Ulvi Yurtsever. This paper was supported in part by National Science Foundation Grant No. AST-8817792.

APPENDIX A: DERIVATION OF EQUATIONS FOR COPLANAR SELF-CONSISTENT SOLUTIONS

In this appendix we derive a complete set of equations that govern self-consistent, coplanar solutions with $B < \frac{1}{2}$, R/B small enough to neglect tidal forces, and a single collision that the ball first encounters before any wormhole traversals and encounters the second time after just one traversal. The bottom line of our derivation will be a proof that, to each nonspurious solution of Eqs. (4.2) and (4.3) there corresponds a solution of the complete equations of motion.

Our derivation involves the geometric parameters depicted in Fig. 17, which is a more detailed version of Fig. 11. The first phase of our derivation is to construct a full set of equations of motion. The equations in our full set will be numbered; other equations along the way will be unnumbered. The full set consists of (i) three "main equations," which can be thought of as coupled equations for three unknowns, α, β, and v_2, in terms of the wormhole and ball radii B, R and the parameters v_1, θ, ϕ of the ball's initial trajectory, and (ii) a set of auxiliary equations, which express various geometric parameters appearing in the main equations in terms of the

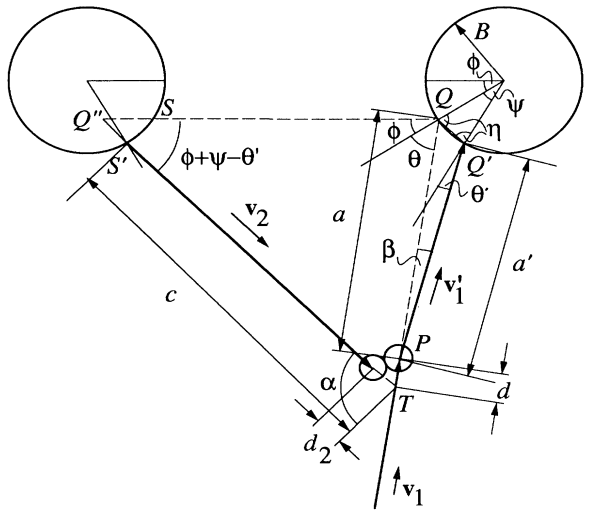

FIG. 17. Full geometry of a self-consistent solution with one wormhole traversal and one billiard-ball collision. This is the same as Fig. 11, but with many more details shown. By convention, all angles and distances (e.g., α, β, d, and d_2) are positive when their orientations are as shown here.

unknowns α, β, v_2 and the knowns B, R, v_1, θ, ϕ.

We begin by constructing the three main equations. They are based on and embody the laws of mirror exchange (which guarantee conservation of momentum and energy), the geometry of the balls relative to each other and relative to their trajectories at the moment of collision, and the demand that the ball return to the event of collision at the same external time T as it left it. (These are all the laws of motion except for the wormhole traversal rules and the law of straight-line motion between collisions and traversal; those remaining laws are embodied in the auxiliary equations.)

The laws of mirror exchange (2.4a) can be rewritten as

$$v_1' = v_2, \quad \mathbf{v}_1' \times (\mathbf{v}_1 + \mathbf{v}_2) = -\mathbf{v}_2 \times (\mathbf{v}_1 + \mathbf{v}_2) ,$$

$$v_2' = v_1, \quad \mathbf{v}_2' \times (\mathbf{v}_1 + \mathbf{v}_2) = -\mathbf{v}_1 \times (\mathbf{v}_1 + \mathbf{v}_2)$$

(together with the requirement that we reject the spurious solutions $\mathbf{v}_1' = -\mathbf{v}_2$, $\mathbf{v}_2' = -\mathbf{v}_1$). The first pair of these determine $\mathbf{v}_1'$ in terms of $\mathbf{v}_1$ and $\mathbf{v}_2$, and will be crucial to our analysis. The second pair determine $\mathbf{v}_2'$, which is of no interest, and thus we can and shall ignore them. The first relation $v_1' = v_2$ we shall automatically use throughout the analysis without even writing it down; i.e., nowhere will v_1' appear; we shall always write v_2 in its place. The second relation $\mathbf{v}_1' \times (\mathbf{v}_1 + \mathbf{v}_2) = -\mathbf{v}_2 \times (\mathbf{v}_1 + \mathbf{v}_2)$, which then becomes our sole embodiment of mirror exchange and hence of energy and momentum conservation, we rewrite in terms of the speeds and angles shown in Fig. 17:

$$v_2 \sin(\alpha - \beta) = v_1(\sin\alpha + \sin\beta) .$$

In order to free this equation from its spurious solution $\alpha - \beta = \pi$ (i.e., $\mathbf{v}_1' = -\mathbf{v}_2$), we divide both sides by $2\cos\frac{1}{2}(\alpha - \beta)$, thereby obtaining

$$v_2 \sin\tfrac{1}{2}(\alpha - \beta) = v_1 \sin\tfrac{1}{2}(\alpha + \beta) . \tag{A1}$$

This is our first main equation.

Turn, next, to the geometry of the collision. Letting the collision occur at time $T = 0$ and introducing a suitable origin of coordinates, we can write the incoming trajectories as

$$\mathbf{r}_1(T) = \mathbf{v}_1 T, \quad \mathbf{r}_2(T) = \mathbf{v}_2 T - 2sR\frac{\mathbf{v}_1 + \mathbf{v}_2}{|\mathbf{v}_1 + \mathbf{v}_2|} ;$$

cf. Eq. (2.4b). These two trajectories intersect spatially ($\mathbf{r}_1 = \mathbf{r}_2$) at times $T_1 = -d/v_1$ and $T_2 = d_2/v_2$, where d and d_2 are the distances shown in Fig. 17. By equating the above expressions for $\mathbf{r}_1(T_1)$ and $\mathbf{r}_2(T_2)$, we obtain

$$\frac{\mathbf{v}_2}{v_2} d_2 + \frac{\mathbf{v}_1}{v_1} d = 2sR\frac{\mathbf{v}_1 + \mathbf{v}_2}{|\mathbf{v}_1 + \mathbf{v}_2|} .$$

By forming the scalar products of this equation with $\mathbf{v}_1 - v_2^{-2}(\mathbf{v}_1 \cdot \mathbf{v}_2)\mathbf{v}_2$ (i.e., the component of $\mathbf{v}_1$ orthogonal to $\mathbf{v}_2$), and with $\mathbf{v}_2 - v_1^{-2}(\mathbf{v}_2 \cdot \mathbf{v}_1)\mathbf{v}_1$ (i.e., the component of $\mathbf{v}_2$ orthogonal to $\mathbf{v}_1$), we obtain several important relations: (i) our second main equation

$$|d|/v_1 = 2R/|\mathbf{v}_1 + \mathbf{v}_2| = 2R/(v_1^2 + v_2^2 + 2v_1 v_2 \cos\alpha)^{1/2} ; \tag{A2}$$

(ii) the relation

$$d_2/v_2 = d/v_1 ,$$

which we shall use below to eliminate d_2 from our third main equation; and (iii) the signs of d and d_2

$$\mathrm{sign}(d_2) = \mathrm{sign}(d) = s .$$

[Recall that s was originally defined as the sign of $v_2 - v_1$; cf. Eq. (2.4b).] These signs are also the same as that of β,

$$\mathrm{sign}(\beta) = \mathrm{sign}(d) = s$$

[a relation embodied in the text's Eq. (4.6c)], as one can see from the following: The geometry of any collision dictates that the momentum transferred to ball 1 be along the line of centers from ball 2 to ball 1, i.e., $\mathbf{v}_1' - \mathbf{v}_1 \uparrow\uparrow \mathbf{r}_1 - \mathbf{r}_2$ (where $\uparrow\uparrow$ means "points in the same direction as"). Combining this with Eq. (2.4b), we see that $\mathbf{v}_1' - \mathbf{v}_1 \uparrow\uparrow s(\mathbf{v}_2 + \mathbf{v}_1)$. Taking the cross product with $\mathbf{v}_1$ we see that $\mathbf{v}_1' \times \mathbf{v}_1 \uparrow\uparrow s\mathbf{v}_2 \times \mathbf{v}_1$, which with the aid of Fig. 17 (and the fact that always $\sin\alpha > 0$) implies that $\sin\beta = s$.

Consider, next, the law that the total time lapse between the ball's first and second encounters with the collision must vanish. From Fig. 17, we see that the vanishing total time lapse is given by the time needed to travel the distances a' and $c - d_2$ both at speed v_2, *minus* the time delay $\Delta T = 1$ introduced by the wormhole traversal:

$$\frac{a'}{v_2} + \frac{c - d_2}{v_2} - 1 = 0 .$$

Using the preceding equation to eliminate d_2, we obtain

our third main equation:

$$v_2 = \frac{a' + c}{1 + d/v_1} \ . \tag{A3}$$

The auxiliary equations, which embody the laws of straight-line motion between collisions and wormhole traversal, and also embody the wormhole traversal rules, are

$$c = \frac{\sin(\theta+\phi)}{\sin\alpha}\left(1 - 2B\cos\phi + 2B\frac{\sin(\psi/2)\cos\gamma_1}{\sin\gamma_2}\right) - 2B\frac{\sin(\psi/2)\cos\gamma_3}{\sin\gamma_2} \ , \tag{A4}$$

$$d = -a + \frac{\sin\gamma_2}{\sin\alpha}\left(1 - 2B\cos\phi + 2B\frac{\sin(\psi/2)\cos\gamma_1}{\sin\gamma_2}\right) \ , \tag{A5}$$

$$a = \frac{B}{\sin\beta}[\sin(\theta-\beta) - \sin\theta'] \ , \tag{A6}$$

$$a' = a\frac{\cos[(\theta+\beta+\theta')/2]}{\cos[(\theta-\beta+\theta')/2]} \ , \tag{A7}$$

$$\psi = \theta - \beta - \theta' \ , \tag{A8}$$

$$\gamma_1 = \tfrac{1}{2}(\theta - 3\theta' - \beta) \ , \tag{A9}$$

$$\gamma_2 = \theta + \phi - 2\theta' - \beta \ , \tag{A10}$$

$$\gamma_3 = \tfrac{1}{2}(\theta - \theta' - \beta) + \phi \ , \tag{A11}$$

$$\theta' = \phi + \theta - \frac{\alpha+\beta}{2} \ , \tag{A12}$$

These auxiliary equations can be derived as follows:

It should be clear from Fig. 17 that $\overline{PQ} = a$ and $\overline{PQ'} = a'$, and that Q and Q' form an isosceles triangle with the center of the right-hand wormhole mouth. Hence, $\overline{QQ'} = 2B\sin(\psi/2)$ and $\eta = (\pi - \psi)/2$. The interior angles of the triangle PQQ' must add up to π:

$$\beta + (\pi - \eta - \theta) + (\pi - \eta + \theta') = \pi \ .$$

When η is reexpressed in terms of ψ, this immediately becomes Eq. (A8). Furthermore, applying the sine theorem to the triangle PQQ' yields (i) the relation

$$\frac{a}{\sin(\pi - \eta + \theta')} = \frac{a'}{\sin(\pi - \eta - \theta)} \ ,$$

which implies Eq. (A7); and (ii)

$$\frac{a}{\sin(\pi - \eta + \theta')} = \frac{2B\sin(\psi/2)}{\sin\beta} \ ,$$

which implies

$$2\sin[(\theta - \beta - \theta')/2]\cos[(\theta - \beta + \theta')/2] = \frac{a}{B}\sin\beta \ ,$$

which, by a well-known trigonometric formula, implies Eq. (A6).

Summing up the interior angles of the triangle TQQ'', we find

$$(\phi + \psi - \theta') + (\phi + \theta) + (\pi - \alpha) = \pi \ ,$$

which, when Eq. (A8) is used, yields Eq. (A12). Figure 18 expands on some details of Fig. 17. Applying the sine theorem to the triangle $Q''SS'$, we find

$$l_1 = 2B\sin(\psi/2)\frac{\sin(\eta + \theta')}{\sin(\phi + \psi - \theta')}$$

and

$$l_2 = 2B\sin(\psi/2)\frac{\sin(\eta - \phi)}{\sin(\phi + \psi - \theta')} \ .$$

For the triangle TQQ'' the sine theorem implies

$$c + l_2 = (1 - 2B\cos\phi + l_1)\frac{\sin(\phi+\theta)}{\sin(\pi - \alpha)}$$

and

$$a + d = (1 - 2B\cos\phi + l_1)\frac{\sin(\phi + \psi - \theta')}{\sin(\pi - \alpha)} \ ,$$

where we have used the relation $\overline{SQ} = 1 - 2B\cos\phi$. If, in the last two equations, we eliminate l_1, l_2, η, and ψ by using the relations found so far, we obtain Eqs. (A4) and (A5) with the auxiliary definitions (A6)–(A11). This completes our derivation of the auxiliary equations (A4)–(A12).

The next phase of our analysis is a derivation of the

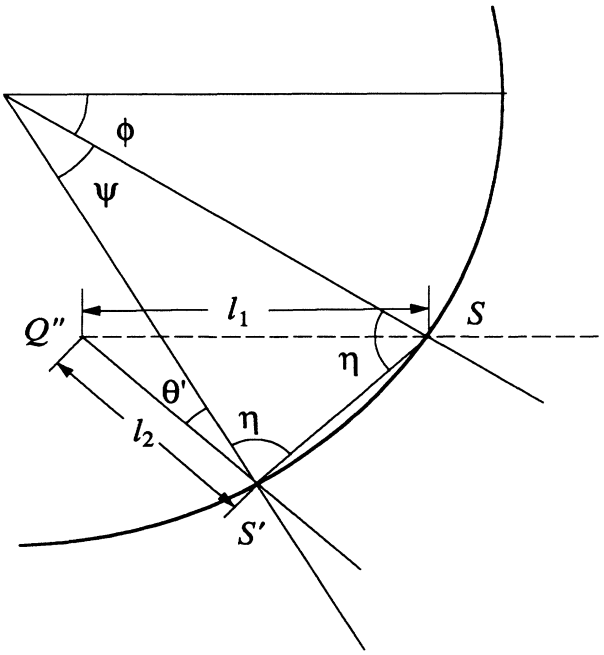

FIG. 18. Some details of Fig. 17 near the wormhole's left mouth (mouth 1).

text's equations (4.2) and (4.3) for the angles α and β. These coupled equations follow from our main and auxiliary equations in the following manner: First we define

$$\rho \equiv v_2/v_1 \ , \tag{A13}$$

and reexpress Eq. (A1) as

$$\rho = \frac{\sin[\frac{1}{2}(\alpha+\beta)]}{\sin[\frac{1}{2}(\alpha-\beta)]} \ . \tag{A14}$$

Now, using Eq. (A2) d can be expressed in terms of ρ and α as

$$d = 2sR/(1+\rho^2+2\rho\cos\alpha)^{1/2} \ , \tag{A15}$$

where $s = \mathrm{sign}(d)$. By combining Eqs. (A7), (A6), and (A12), it can be shown that

$$\begin{aligned} a'\sin\beta &= B[\sin\theta - \sin(\beta+\theta')] \\ &= B\left[\sin\theta - \sin\left(\theta+\phi-\frac{\alpha-\beta}{2}\right)\right] \ . \end{aligned} \tag{A16}$$

From Eqs. (A9)—(A11) it can be seen that $\gamma_2 = \gamma_1 + \gamma_3$, and from (A10) and (A12) that $\alpha = \theta + \phi + \gamma_2$. Using these in Eq. (A4), one can show that

$$\begin{aligned} c\sin\alpha &= \sin(\theta+\phi)(1-2B\cos\phi) \\ &\quad -2B\sin(\psi/2)\cos(\theta+\phi+\gamma_3) \ . \end{aligned} \tag{A17}$$

Next, using (A12) in (A8)–(A11), we obtain all the auxiliary angles in terms of α and β:

$$\begin{aligned} &\psi = -\phi + \tfrac{1}{2}(\alpha-\beta), \quad \gamma_1 = -\theta - \tfrac{3}{2}\phi + \tfrac{3}{4}\alpha + \tfrac{1}{4}\beta \ , \\ &\gamma_2 = \alpha - \theta - \phi, \quad \gamma_3 = \tfrac{1}{2}\phi + \tfrac{1}{4}(\alpha-\beta) \ . \end{aligned} \tag{A18}$$

Using these expressions and some trigonometric manipulations, Eq. (A17) can be simplified further, giving

$$\begin{aligned} c\sin\alpha &= \sin(\theta+\phi) \\ &\quad -B\left[\sin\left(\theta+\phi+\frac{\alpha-\beta}{2}\right)+\sin\theta\right] \ . \end{aligned} \tag{A19}$$

Finally, eliminating v_2 between (A13) and (A3), and replacing ρ, a', and c from (A14), (A16), and (A19), we obtain the first of our equations for α and β: Eq. (4.2); and we obtain the second, Eq. (4.3) by eliminating a between (A5) and (A6), using the values (A18) and (A12) of the auxiliary angles, and performing some algebraic manipulations.

Notice that, in the process of deriving our two equations (4.2) and (4.3), we multiplied them by $\sin\alpha\sin\beta\sin[(\alpha-\beta)/2]$ [Eq. (4.2)], and by $\sin\alpha\sin\beta$ [Eq. (4.3)]. This introduced the first four spurious solutions of Eq. (4.6a). The fifth spurious solution in (4.6a) is the self-inconsistent solution. Since v_2 and v_1 are both positive by definition, $\rho \equiv v_2/v_1$ must also be positive, so any solution for α and β which produces a negative ρ via Eq. (A14), or equivalently via (4.4a), must be spurious. This accounts for Eq. (4.6b). Finally, as was discussed following Eq. (A2), the collision geometry rules out as spurious any solutions with $\mathrm{sign}(\beta) \neq \mathrm{sign}(d)$, which accounts for Eq. (4.6c).

The last phase of our analysis is to explain why, to every nonspurious solution of Eqs. (4.2) and (4.3) for α and β, there exists a full solution of the billiard ball's equations of motion. The reason is that (i) the main and auxiliary equations (A1)—(A12) embody all the equations of motion (as well as a lot of geometrical constructions); and (ii) by regarding the auxiliary equations (A4)—(A12) and the third main equation (A3) as definitions of other variables in terms of α, β, B, R, v_1, θ, ϕ, and by inserting a nonspurious solution of (4.2) and (4.3) into these equations, we automatically produce a solution of the remaining two main equations (A2) and (A1).

APPENDIX B: SELF-CONSISTENT SOLUTIONS FOR $B \ll 1$

In this appendix we derive the properties of self-consistent solutions quoted in Sec. IV C, for a wormhole and ball with $B \ll 1$ and $R/B < \frac{1}{2}$. We restrict attention to dangerous initial trajectories in the range (4.7) [interior of the dangerous triangle depicted in Fig. 12], and restrict our search to self-consistent solutions with a single collision of the type shown in Fig. 17 and with $|\beta| \ll 1$ and $|\varepsilon| \ll 1$, where $\varepsilon \equiv \alpha - 2\phi$; cf. Eqs. (4.9).

We begin our derivation in Appendix B 1 by expanding the highly nonlinear, coupled equations (4.2), (4.3) in powers of β and ε to the leading orders that produce nonspurious solutions. Then in Appendix B 2 we derive explicit solutions to those approximate equations for the central region of the dangerous triangle, and in Appendix B 3 for the upper-edge region of the triangle.

1. Approximate equations

In this section we derive the approximate equations for β and ε by power-series expansions of Eqs. (4.2) and (4.3). To facilitate the expansion of Eq. (4.2), we first divide it by $\sin(\alpha/2)$ (a factor that appears in each term in the limit of vanishing β). When we then expand, the resulting equations are homogeneous in β and ε and at linear order admit only spurious solutions, so we move on to quadratic order. Up through quadratic order the expanded equations take the forms

$$M\varepsilon + N\varepsilon^2 + P_1\beta + Q_1\beta^2 + S_1\beta\varepsilon = 0 \ , \tag{B1}$$

$$M\varepsilon + N\varepsilon^2 + P_2\beta + Q_2\beta^2 + S_2\beta\varepsilon = 0 \ , \tag{B2}$$

for which the coefficients M and N of ε and ε^2 are identically the same in the two equations. The expressions for all the expansion coefficients are

$$M = \tfrac{1}{2}B\sin 2\phi\cos\theta \ , \tag{B3}$$

$$N = \tfrac{1}{2}B(\cos 2\phi\cos\theta + \tfrac{1}{4}\sin 2\phi\sin\theta) \ , \tag{B4}$$

$$\begin{aligned} P_1 &= -\sin(\phi-\theta) - 2(4\lambda_1+s-2)R\sin\phi \\ &\quad + B\left[\tfrac{3}{4}\sin(2\phi-\theta) - \tfrac{1}{4}\sin(2\phi+\theta) - \sin\theta\right] \ , \end{aligned} \tag{B5}$$

$$Q_1 = -\cos\phi\cos\theta - \tfrac{1}{2}\cot\phi\sin(\phi+\theta) - 2(2\lambda_1-1)R\cos\phi + B[\tfrac{1}{2}(9\cos^2\phi-1)\cos\theta + \tfrac{1}{4}\sin\theta\cot\phi(7\cos^2\phi-3)] , \quad \text{(B6)}$$

$$S_1 = -\cos 2\phi\cos\theta/\cos\phi + R[2(2\lambda_1-1)/\cos\phi + (4-8\lambda_1-s)\cos\phi] + B[\cos\theta(\tfrac{3}{2}\cos^2\phi-1) + \tfrac{1}{4}\sin 2\phi\sin\theta] , \quad \text{(B7)}$$

$$P_2 = -\sin(\phi-\theta) + 2sR\sin\phi + B(-2\sin\theta\cos^2\phi + \tfrac{1}{2}\sin 2\phi\cos\theta) , \quad \text{(B8)}$$

$$Q_2 = -sR\cos\phi + B(\tfrac{1}{2}\cos\theta - \tfrac{3}{8}\sin 2\phi\sin\theta) , \quad \text{(B9)}$$

$$S_2 = -\cos(\phi-\theta) + sR\cos\phi + B(\cos\theta\cos^2\phi + \tfrac{5}{4}\sin\theta\sin 2\phi) . \quad \text{(B10)}$$

Here the notation is that of Sec. IV and Appendix A, including the use of λ_1 as a surrogate for the ball's initial speed v_1; cf. Eqs. (4.10) and (4.8) which imply

$$v_1 = \frac{1}{\cos\phi}[(1-2B\cos\phi)\cos\theta + 2R(2\lambda_1-1)] . \quad \text{(B11)}$$

By subtracting Eq. (B2) from Eq. (B1) and dividing by β, we obtain the linear equation

$$Q\beta + S\varepsilon + P = 0 , \quad \text{(B12)}$$

where

$$Q = -\cos\phi\cos\theta - \tfrac{1}{2}\cot\phi\sin(\phi+\theta) - (4\lambda_1 - s - 2)R\cos\phi + B(-\cos\theta + \tfrac{9}{2}\cos^2\phi\cos\theta + \cos^2\phi\cot\phi\sin\theta) , \quad \text{(B13)}$$

$$S = \cos\theta/\cos\phi - \cos(\phi+\theta) + R[2(1-2\lambda_1)\cos 2\phi/\cos\phi - 2s\cos\phi] + B(-\cos\theta + \tfrac{1}{2}\cos\theta\cos^2\phi - \sin 2\phi\sin\theta) , \quad \text{(B14)}$$

$$P = -4R\sin\phi(2\lambda_1 + s - 1) . \quad \text{(B15)}$$

We shall use Eqs. (B2) and (B12) as our approximate, coupled equations for β and ε. Since one is quadratic and the other is linear, they can be combined to form a single quadratic equation for β or for ε, but the coefficients in that quadratic equation are so complicated that we shall not write it down explicitly except in special regimes where the coefficients simplify.

The coefficients in our quadratic and linear equations (B2) and (B12) change drastically (because $R \ll 1$ and $B \ll 1$) as one approaches the edges of the dangerous triangle (Fig. 12), $\phi - \theta \to 0$, $\phi + \theta \to B$, $\phi \to \pi/2$. Correspondingly, the structures of the solutions change drastically as one approaches the edges. In Appendix B 2 we shall consider the central region (extending out to the right edge), and in Appendix B 3, the upper-left-edge region. Near the lower left edge and the left corner, ε grows large, invalidating the power-series expansion that underlies our quadratic and linear equations (B2) and (B12), and thus the methods of this appendix are not usable there.

2. Solutions in the central region

We specialize, now, to the central region of the dangerous triangle, $\phi-\theta \gg B$, $\phi+\theta-B \gg R$; and we retain our previous assumptions, $B \ll 1$, $R/B < \frac{1}{2}$. In one of our manipulations we shall require an additional constraint: $\varepsilon \ll \phi - \theta$. Since $\phi - \theta \gg B$ and ε has already been assumed small, this additional constraint is not severe.

These constraints on the parameters imply that in (B2) the terms in ε^2, β^2, and $\beta\varepsilon$ can be neglected compared to the first-order terms. The result is the linear relation

$$\beta = \frac{\sin 2\phi\cos\theta}{2\sin(\phi-\theta)}B\varepsilon \ll \varepsilon . \quad \text{(B16)}$$

Inserting this relation into our linear equation (B12), we find that ε is (very nearly) independent of B:

$$\varepsilon = \frac{8\cos\phi}{\sin(\theta+\phi)}(\lambda_1 - \sigma)R , \quad \text{(B17)}$$

with

$$\sigma \equiv \tfrac{1}{2}(1-s) = \begin{cases} 0 & \text{if } s = +1 , \\ 1 & \text{if } s = -1 . \end{cases} \quad \text{(B18)}$$

Inserting this back into Eq. (B16), we obtain

$$\beta = \frac{4\sin 2\phi\cos\phi\cos\theta}{\sin(\phi-\theta)\sin(\phi+\theta)}(\lambda_1-\sigma)BR = \frac{8\sin\phi}{\cos\theta(\tan^2\phi - \tan^2\theta)}(\lambda_1-\sigma)BR , \quad \text{(B19)}$$

and by inserting these relations into Eqs. (A13), (A14), and (4.11), we obtain the dimensionless parameter λ_2 that describes the speed v_2 of the ball between its encounters with the collision

$$\lambda_2 - \sigma = \left[1 + \frac{\cos^3\phi\cos^2\theta}{2\sin(\phi-\theta)\sin(\phi+\theta)}B\right](\lambda_1-\sigma) = \left(1 + \frac{2\cos\phi}{\tan^2\phi - \tan^2\theta}B\right)(\lambda_1-\sigma) . \quad \text{(B20)}$$

Equations (B17)–(B20) are the simple form of the solutions for self-consistent collisions of class I ($s = +1$, $\sigma = 0$) and class II ($s = -1$, $\sigma = 1$), which we quoted and discussed in Sec. IV B [Eqs. (4.14) and (4.15)].

3. Solutions in the upper-edge region

We turn, finally, to the upper-left-edge region of the dangerous triangle, $0 \le \phi - \theta \lesssim B$; and in order to obtain valid solutions with $|\beta| \ll 1$ and $|\varepsilon| \ll 1$, we bound ourselves away from the triangle's left corner—i.e., we assume that $\phi \gg B$. In our formulas we shall characterize the difference $\phi - \theta$ by a dimensionless parameter

$$\mu \equiv (\phi - \theta)/B . \quad \text{(B21)}$$

As in the preceding subsection, our constraints on ϕ and θ make the ε^2 and β^2 terms in Eq. (B2) negligible compared to the first-order terms; but now the $\beta\varepsilon$ term is not *a priori* negligible. As a result, Eq. (B2) takes the form

$$k_1\beta + k_2\varepsilon + k_3\beta\varepsilon = 0 \ , \tag{B22}$$

where

$$k_1 = -\mu B + 2sR\sin\phi - B\sin\phi\cos^2\phi \ , \tag{B23}$$

$$k_2 = B\sin\phi\cos^2\phi \ , \tag{B24}$$

$$k_3 = -1 \ . \tag{B25}$$

Our other, linear, equation for ε and β [Eq. (B12)] also simplifies; its coefficients become

$$Q = -2\cos^2\phi \ , \tag{B26}$$

$$S = 2\sin^2\phi \ , \tag{B27}$$

$$P = -8R\sin\phi(\lambda_1 - \sigma) \ . \tag{B28}$$

By combining our two equations and eliminating ε, we obtain the following quadratic equation for β:

$$\beta^2 + p\beta + q = 0 \ , \tag{B29}$$

with

$$p = 2\tan^2\phi[2(\lambda_1 - \sigma) - s\sin\phi]R - (\sin\phi\cos 2\phi - \mu\tan^2\phi)B \ , \tag{B30}$$

$$q = -4BR\sin^2\phi(\lambda_1 - \sigma) \ . \tag{B31}$$

In discussing the solutions of this quadratic equation we shall restrict attention to the region $0 < \lambda_1 < 1$ of dangerous initial trajectories.

By examining the signs of the coefficients in Eq. (B29), it is easy to see that when $s = +1$ (class-I collision) there always exist two real solutions for β, one positive and thus acceptable; the other negative and thus spurious (recall that $\beta > 0$ for class I and $\beta < 0$ for class II; cf. Fig. 3). On the other hand, when $s = -1$ there is always a range of ϕ where $p^2/4 - q < 0$ and there is no solution. For $R \ll 1$ and $\mu \ll 1$, this no-solution region is $\phi \sim \pi/4$.

Focus attention on the always existent class-I solution, $s = +1$ (and $\sigma = 0$). Since $q < 0$ in this case, the solution is

$$\beta = -p/2 + \sqrt{p^2/4 - q} \ . \tag{B32}$$

When one continuously varies ϕ in the range of our analysis, $\phi \gg B$, p passes through 0 at some point and changes sign. Since q is second order in the small radii B and R, while p is first order, there is a sharp change in the form of the solution (B32) at that point:

$$\beta = \begin{cases} -q/p & \text{if } p \gg |q| \ , \\ -p & \text{if } p \ll -|q| \ . \end{cases} \tag{B33}$$

When $R\tan^2\phi \ll B$ and $\mu\tan^2\phi \ll 1$, the change of sign for p occurs very close to $\pi/4$, and the solution (B33) on the two sides of $\pi/4$ is

$$\beta = \sin\phi\cos 2\phi B, \quad \varepsilon = \frac{\cos 2\phi\cos^2\phi}{\sin\phi}B \quad \text{if } \phi - \pi/4 \ll -R\lambda_1 \ , \tag{B34}$$

and

$$\beta = \varepsilon = -\frac{4\sin\phi}{\cos 2\phi}R\lambda_1 \quad \text{if } \phi - \pi/4 \gg +R\lambda_1 \ . \tag{B35}$$

Notice that in (B34) β and ϕ are independent of λ_1, while in (B35) they are proportional to it. These are the solutions quoted in Eqs. (4.14) and (4.15).

[1] M.S. Morris, K.S. Thorne, and U. Yurtsever, Phys. Rev. Lett. **61**, 1446 (1988).

[2] V.P. Frolov and I.D. Novikov, Phys. Rev. D **42**, 1057 (1990); see also I.D. Novikov, Zh. Eksp. Teor. Fiz. **95**, 769 (1989) [Sov. Phys. JETP **68**, 439 (1989)].

[3] S.-W. Kim and K.S. Thorne, Phys. Rev. D **43**, 3929 (1991).

[4] V.P. Frolov, Phys. Rev. D **43**, 3878 (1991); U. Yurtsever, Class. Quantum Grav. **8**, 1127 (1991).

[5] G. Klinkhammer, Phys. Rev. D **43**, 2542 (1991); U. Yurtsever, Class. Quantum Grav. Lett. **7**, L251 (1990); R.M. Wald and U. Yurtsever, Phys. Rev. D **44**, 403 (1991).

[6] J. Friedman, M.S. Morris, I.D. Novikov, F. Echeverria, G. Klinkhammer, K.S. Thorne, and U. Yurtsever, Phys. Rev. D **42**, 1915 (1990); cited in text as "the consortium."

[7] J. Friedman and M.S. Morris, Phys. Rev. Lett. **66**, 401 (1991); and (in preparation).

[8] U. Yurtsever, J. Math. Phys. **31**, 3064 (1990).

[9] G. Klinkhammer and K.S. Thorne (in preparation); cited in text as paper II.

[10] I.D. Novikov and V. Petrova (research in progress).

[11] I.D. Novikov (unpublished).

[12] R.L. Forward conceived this example for use in his forthcoming science fiction novel, Timemaster.

[13] M. Morris and K.S. Thorne, Am. J. Phys., **56**, 395 (1988).